ENHANCING ROLL STABILITY AND DIRECTIONAL PERFORMANCE OF ARTICULATED HEAVY VEHICLES BASED ON ANTI-ROLL CONTROL AND DESIGN OPTIMIZATION

by

Dhruv Oberoi

A thesis presented to the

University of Ontario Institute of Technology

in the fulfillment of the

thesis requirement for the degree of

Master of Applied Science

in

Automotive Engineering

Oshawa, Ontario, Canada, 2011

AUTHOR'S DECLERATION

I hereby declare that I am the sole author of this thesis. This is a true copy of the thesis, including any required final revisions, as accepted by my examiners.

I understand that my thesis may be made electronically available to the public.

ABSTRACT

This research presents an investigation to actively improve the rollover stability of articulated heavy vehicles (AHVs) during high speed manoeuvres using anti-roll control systems. A 3-dimensional (3-D) linear yaw/roll model with 5 degrees of freedom is developed. Based on this model a linear quadratic regulator (LQR) controller is designed to improve the rollover stability of a tractor/semi-trailer combination. A design optimization method for AHVs using genetic algorithms (GAs) and multibody vehicle system models is also presented. AHVs have poor manoeuvrability when travelling at low speeds on local roads and city streets. On the other hand, these vehicles exhibit unstable motion modes at high speeds, including jack-knifing, trailer sway and rollover. From the design point of view, the low-speed manoeuvrability and high-speed stability have conflicting requirements on some design variables. The design method based on a GA and a multibody vehicle dynamic package, TruckSim, is proposed to coordinate this trade-off relationship. To test the effectiveness of the design method, a tractor/semi-trailer combination is optimized using the proposed method. It is demonstrated that the proposed design method can be used for identifying desired design variables and predict performance envelopes in the early design stages of AHVs.

ACKNOWLEDGEMENTS

I am deeply grateful to my supervisor Dr. Yuping He for his unflagging encouragement, guidance and support during this research. I would like to thank my supervisory committee members Dr. Ebrahim Esmailzadeh and Dr. Ghaus M. Rizvi for serving on my thesis committee and making significant contribution to enhance the quality of this work. I would like to thank Dr. George Zhu for also serving on my thesis defense committee and making significant contributions to enhance the quality of this work. I would also like to thank my family and all my good friends at UOIT, whose friendship and support throughout this research was invaluable. Financial support of this research by the Natural Science and Engineering Research Council of Canada and Canadian Foundation for Innovation is gratefully acknowledged.

DEDICATION

I would like to dedicate this work to my parents and elder brother for their unconditional love and affection and unremittingly encouraging and supporting me in all my endeavors. Above all I dedicate this work to the Almighty as he perpetually showers his blessings on us.

CONTENTS

LIST OF FIGURES

LIST OF TABLES

NOMENCLATURE

Subscripts and Superscripts

$\square_i$ variable of the i^{th} unit of the articulated heavy vehicle

For the vehicle of tractor semitrailer; 1 – tractor and 2 – semitrailer

$\dot{\square}$ first time derivative of variable

$\ddot{\square}$ second time derivative of variable

Upper Case Notations

A, B, C matrices of continuous-time state-space representation

I_{xxi} roll moment of inertia of the vehicle unit i^{th} sprung mass, measured about the CG of sprung mass

I_{xzi} roll/yaw product of inertia of the vehicle unit i^{th} sprung mass, measured about the CG of sprung mass

I_{zzi} yaw moment of inertia of the vehicle unit i^{th} sprung mass, measured about the CG of whole vehicle mass

J cost function of optimal control

K vector gains in the optimal control

K_{12} roll stiffness of coupling point of tractor and semitrailer

K_{f1} auxiliary roll stiffness of front suspension of tractor

K_{r1} auxiliary roll stiffness of rear suspension of tractor

K_{r2} auxiliary roll stiffness of rear suspension of semitrailer

K_{tf1} combined roll stiffness of tractor front axle tires

K_{tr1} combined roll stiffness of tractor rear axle tires

K_{tr2} combined roll stiffness of semitrailer tridem tires

L_{f1} auxiliary roll damping of tractor front suspension

L_{r1} auxiliary roll damping of tractor rear suspension

L_{r2} auxiliary roll damping of semitrailer rear suspension

$N_{\beta i}$ $\frac{\partial M_z}{\partial \beta_i} = \sum_j x_{i,j} C_{\alpha ij}$

partial derivative of net tire yaw moment of the vehicle i^{th} unit w.r.t. sideslip angle

$N_{\delta lf}$ $\frac{\partial M_z}{\partial \delta_{1f}} = -x_{1f} C_{\alpha 1f}$

partial derivative of net tire yaw moment of tractor front axle w.r.t. steer angle

N_{ri} $\frac{\partial M_z}{\partial r_i} = \sum_j \frac{{l_{i,j}}^2 C_{\alpha ij}}{u_i}$

partial derivative of net tire yaw moment of the vehicle i^{th} unit w.r.t. yaw rate

Q weighting matrix on vehicle states in optimal control

R weighting matrix on vehicle roll in optimal control

$Y_{\beta i}$ $\frac{\partial M_z}{\partial \beta_i} = \sum C_{\alpha ij}$ (j^{th} axle on the vehicle unit i)

partial derivative of net tire lateral force of the vehicle i^{th} unit w.r.t. sideslip angle

$Y_{\delta lf}$ $\frac{\partial M_z}{\partial \delta_{1f}} = -C_{\alpha 1f}$

partial derivative of net tire lateral force of tractor front axle w.r.t. steer angle

Y_{ri} $\frac{\partial M_z}{\partial r_i} = \sum_j \frac{{l_{i,j}}^2 C_{\alpha ij}}{u_i}$

partial derivative of net tire lateral force of the vehicle i^{th} unit w.r.t. yaw rate

Lower Case Notations

a_1 distance between front wheel centre and CG of tractor

a_2 distance between hitch centre and CG of semitrailer

b_1 distance between rear wheel centre and CG of tractor

b_2 distance between tridem middle wheel centre and CG of semitrailer

c_{f1} combined cornering stiffness of tractor front axle tires

c_{r1} combined cornering stiffness of tractor rear axle tires

c_{r2} combined cornering stiffness of semitrailer tridem tires

g acceleration due to gravity

h_{ci} height of coupling point of the vehicle i^{th} unit, measured upward from ground

h_{cri} height of coupling point of the vehicle i^{th} unit, measured upward from its roll axis

h_{ri} height of roll axis of the vehicle i^{th} unit, measured upward from ground

h_{si} height of sprung mass CG of the vehicle i^{th} unit, measured upward from ground

l_i wheelbase of the vehicle i^{th} unit

l_{ci} distance between the whole mass CG of the vehicle i^{th} unit and the coupling point

m_i total mass of the vehicle i^{th} unit

m_{s1} sprung mass of the vehicle i^{th} unit

m_{ui} unsprung mass of the i^{th} axle from the vehicle front

t_i track of the i^{th} axle from the vehicle front

u control input in optimal control

u_i longitudinal velocity of the vehicle i^{th} unit

x vector of linear vehicle states

Symbolic Notations

β_i sideslip angle of vehicle body of the vehicle i^{th} unit

Γ articulation angle between tractor and semitrailer

δ_{1f} steer angle of tires on the front axle of tractor

Φ_i absolute roll angle of sprung mass of the vehicle i^{th} unit

Ψ_i yaw angle of vehicle body of the vehicle i^{th} unit

ABBREVIATIONS

AHV	articulated heavy vehicle
ARSC	anti roll stability control
DOF	degree of freedom
GA	genetic algorithm
LCV	long combination vehicle
LQR	linear quadratic regulator
MPC	model predictive control
PFOT	path following off-tracking
RWA	rearward amplification
SAE	society of automotive engineers
SPW_{90}	swept path width 90^0

CHAPTER 1

INTRODUCTION

1.1 WHAT ARE ARTICULATED VEHICLES?

A towing/driving unit and one or more trailing units coupled by one or more articulation joints is known as an articulated vehicle.

1.2 ARTICULATED HEAVY VEHICLE CONFIGURATIONS

An articulated heavy vehicle (AHV) consists of a tractor/truck which through articulation joints is connected to one or more trailing units. The lead unit controlled by the driver usually has one steerable axle. Each of the trailing units is called a trailer. Each vehicle unit is connected to one another by means of mechanical couplings, such as dollies, hitches, pintles and fifth-wheels. A trailer can be broadly classified either as a full-trailer or a semi-trailer. A full-trailer is vertically supported by running gears both at its front and rear ends. A semi-trailer is vertically supported by a running gear at the rear however and its front is vertically supported by its leading unit. Figure 1.1 shows the common vehicle units and hitches used in AHVs [1].

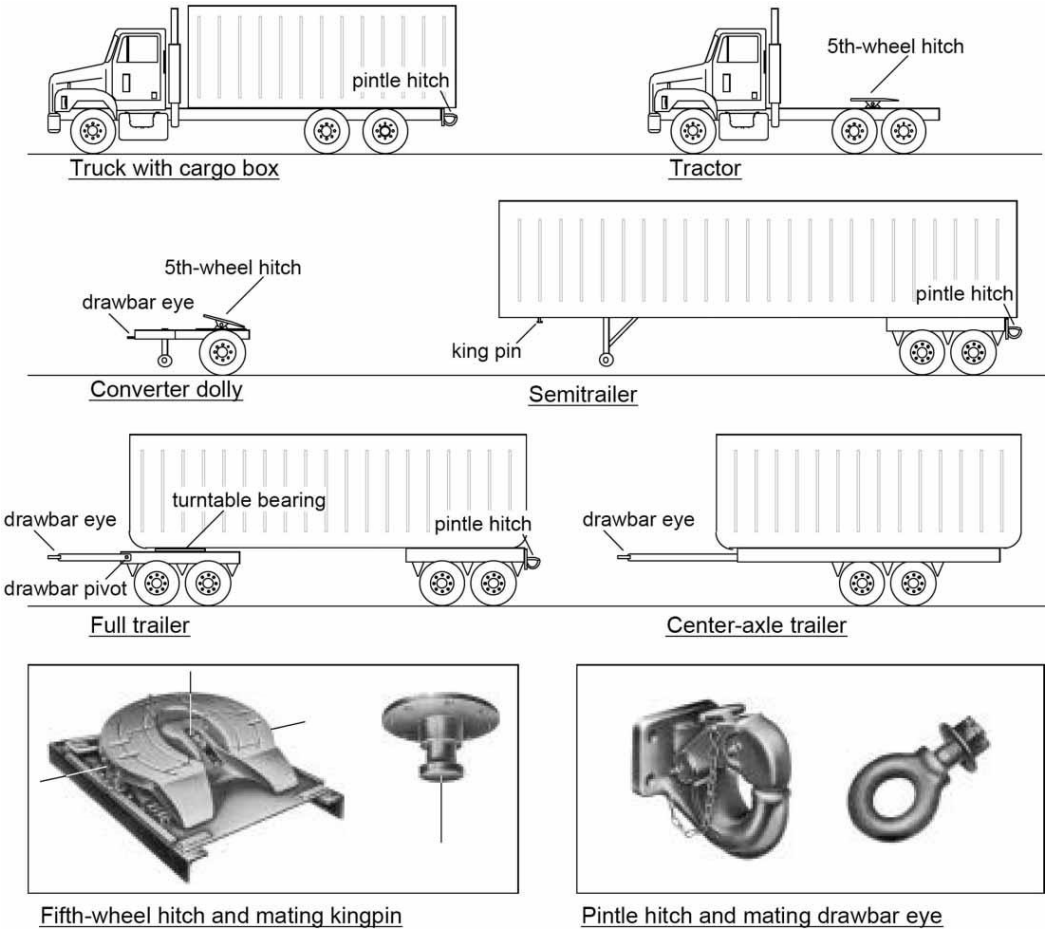

Figure 1.1: Common vehicle units and hitches used in AHVs [1]

1.3 WHY ARE ARTICULATED HEAVY VEHICLES WIDELY USED?

The use of articulated heavy vehicles (AHVs) is steadily increasing every year. This is because AHVs are the most cost-effective and logistically efficient in freight transportation [1]. Compared to a single unit vehicle an AHV transports more freight using a single driver. Also, AHVs have better fuel economy when compared to single unit vehicles [2]. This helps to lower the cost of fuel used to transport the same load of freight and at the same time reduces greenhouse gas emissions. It is because of all

these advantages that AHVs are becoming the preferred mode of transportation of freight all over the world.

1.4 HIGH-SPEED AND LOW-SPEED PERFORMANCE MEASURES OF AHVs

Several researchers have defined high-speed and low-speed performance measures of AHVs based on R*earward Amplification* (RWA) ratio and *Path Following Off-tracking* (PFOT), respectively [5, 21, 35, 55, 67, 68, 69, 70, 73].

1.4.1 HIGH-SPEED PERFORMANCE MEASURE

At high speeds, the lateral stability of AHVs (especially rollover) is mostly dependent on the important high speed dynamic performance measure called *Rearward Amplification* (RWA) ratio [3]. This ratio is defined for an obstacle avoidance manoeuvre [4, 5] and is given as:

$$RWA = \frac{peak\ absolute\ lateral\ acceleration\ at\ rearmost\ unit's\ CG}{peak\ absolute\ lateral\ acceleration\ at\ front\ unit's\ CG} \quad (1.1)$$

Fancher and Winkler [1] signified RWA as the tendency for an articulated vehicle's rearmost unit to have a higher lateral acceleration than that of its front unit.

1.4.2 LOW SPEED PERFORMANCE MEASURE

The trailing units of an AHV exhibit difficulties in following the path of the lead unit during curved path negotiations. Australian performance based standards (PBS) define the low speed manoeuvrability performance of an articulated vehicle by its

Path Following Off-Tracking (PFOT) [6]. It is defined as the maximum radial offset between the path of the vehicle towing unit and that of the rearmost trailing unit as shown in figure 1.2. PFOT has been reported ever since multi-axle vehicles were first built [7].

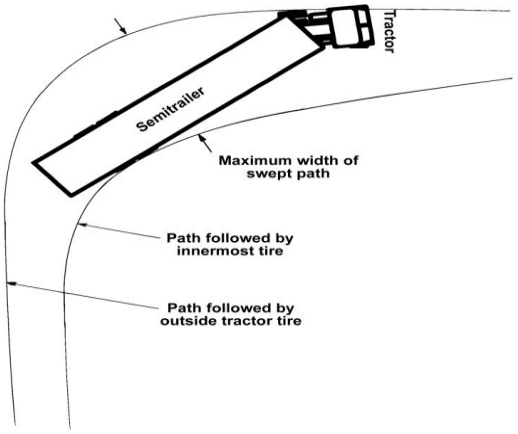

Figure 1.2: Path Following Off-tracking (PFOT) of an AHV [8]

1.5 MOTIVATION

The immense commercial benefits of using AHVs have made them increasingly popular in recent years. It is however reported that poorly designed articulated vehicles tend to suffer from dangerous handling and roll instabilities [9]. Also, an AHV may present unstable motion modes due to its distinguished dynamic features [5]. These unstable motion modes can be classified as; trailer sway, jack-knifing and rollover.

1.5.1 AHV ROLLOVER

The potential of the unstable motion modes of AHVs especially rollover increases at high speeds. Rakheja *et.al.* [10, 11] reported that in Canada almost 40% of the accidents were due to rollover involving tanker vehicles and about 45% of such accidents involving the transportation of dangerous freight. In 2001, a study in the UK reported that 573 heavy vehicle accidents were due to vehicle rollover [12]. It was reported that in 2004 approximately 15000 commercial heavy vehicles were involved in rollover accidents in the US [13]. Most of the articulated vehicle accidents involving rollover occur on highways as reported by Kusters [14].

Rollover accidents can also result in dramatic economical and environmental consequences. In the UK, the cost of rollover accidents can be estimated to be £50 - 100 million annually, excluding environmental costs and those arising from traffic delays [15].

Woodrooffe [16] reported that among all vehicle parameters, a driver's awareness of rollover on existing, non-instrumented vehicles largely depended on vehicle type, torsional stiffness of trailer and the load position. Winkler *et.al.* [17] indicated that drivers of heavy vehicles found it extremely difficult to perceive their proximity to rollover while driving.

Glasner [18] observed that while some of the articulated rollover accidents were preventable given a sophisticated warning system and a highly skilled driver, the majority of these accidents could only be avoided by the intervention of an advanced active safety system. Palkovics *et.al.* [19] reported that almost 50% of the rollovers

accidents considered could not be prevented by driver action alone. This provides compelling motivation to investigate rollover stability enhancement of AHVs owing to safety, environmental consideration and cost reduction involving rollover accidents.

1.5.2 TRADE-OFF BETWEEN HIGH-SPEED AND LOW-SPEED PERFORMANCE OF AHVs

AHVs have poor manoeuvrability when travelling at low speeds on local roads and city streets. On the other hand, these vehicles exhibit unstable motion modes at high speeds, including trailer sway, jack-knifing and rollover. Among all conflicting design goals of AHVs, the trade-off relationship between manoeuvrability at low speeds and lateral stability at high speeds is the most fundamental and important, which bothers vehicle designers and researchers. Due to AHVs' complex configurations and large sizes, as well as limited modeling and simulation tools, the dynamic analysis and design synthesis of these vehicles are mainly based on simplified and linearized 2-dimentional (2-D) yaw plane models. This provides compelling motivation to investigate the coordination of these conflicting design goals.

1.6 THESIS CONTRIBUTIONS

A 3-dimensional (3-D) linear yaw/roll model with 5 degrees of freedom (DOF) is developed. Based on this model, a linear quadratic regulator (LQR) controller is designed to develop an active roll stability control (ARSC) system which actively improves the rollover stability of a tractor/semi-trailer combination.

A design method is proposed to tackle the contradictory design problems of AHVs related to the trade-off between high-speed and low-speed directional

performance. The proposed design method is based on a GA and a multibody vehicle dynamic package, TruckSim. To test the effectiveness of the design method, a tractor semi-trailer combination is optimized using the proposed method.

1.7 THESIS ORGANIZATION

This thesis is organized as follows. Chapter 1 provides general information on AHVs and their applications. Chapter 1 also provides background information on the high speed and low speed performance measures of AHVs. Chapter 2 presents a comprehensive literature review on research related with rollover prevention of AHVs and also on the state of the art of AHV design methodologies. Chapter 3 focuses on the design and analysis tools needed to perform modeling and numerical simulation. The theory of design optimization is discussed with focus on one particular optimization. Also discussed is the basic control theory used in this research. This chapter also describes the various performance indices and test maneuvers for AHVs. Chapter 4 presents an *active roll stability control (ARSC)* system for AHVs. This control system utilizes the *Linear Quadratic Regulator* (LQR) technique and is designed based on a 3-dimensional (3-D) linear yaw/roll model with 5 degrees of freedom (DOF). Chapter 5 presents a design optimization method based on a GA and a multibody vehicle dynamic package, TruckSim, so as to coordinate the trade-off relationship between high-speed and low-speed performance of AHVs. Chapter 6 is the concluding chapter and discusses the achievements of this research and the scope of future research.

CHAPTER 2

LITERATURE REVIEW

2.1 INTRODUCTION

In this chapter a comprehensive literature review is conducted to review researches related with rollover prevention of AHVs and also outline the state of the art of AHV design methodology.

2.2 YAW/ROLL DYNAMICS OF VEHICLES

The safe running of any road vehicle depends on its yaw/roll dynamics. For a single unit vehicle, the loss of yaw stability results in a spin-out. Whereas for an articulated vehicle, the loss of yaw stability leads to either trailer swing or jack-knifing. On the other hand, the loss of roll stability of a vehicle causes a rollover accident.

Some of the most comprehensive general reviews of heavy vehicle dynamics were reported by the University of Michigan Transportation Research Institute [20-22]. Vlk [23, 24] and Nalecz [25] summarized the dynamics of tractor/full-trailer and tractor/semi-trailer combinations. The dynamics of long combination vehicles was reviewed by Segel and Ervin [26] and Ellis [27].

2.2.1 VEHICLE HANDLING DYNAMICS

Handling dynamics is the yaw responses of a vehicle to steering inputs. The handling dynamics of a vehicle is determined by its geometric parameters and the mechanical properties of its suspension, tires and frame [22]. Since the cornering stiffness of pneumatic tires depends on the vertical load, the handling dynamics of a vehicle is highly affected by the change in the weight distribution amongst its axles. The effects of tightly spaced tandem axles and dual tires are also important, but to a smaller level [28]. Pacejka presented the fundamentals of steady state cornering for small passenger vehicles [29, 30] and for bigger and more complex vehicles [31].

The handling dynamics of articulated vehicles is further influenced by interactions between connected vehicle units. The tractor might become more or less understeer depending on the tire cornering stiffness, changes in axle loads and the location of the vehicle couplings. The handling dynamics of the front and trailing units can be characterized as oversteer and understeer. Segel and Ervin [26] reported that the handling instability of a tractor/semi-trailer combination can be classified into three different categories: the combination vehicle will exhibit *trailer swing* when the lead unit is oversteer and the trailing unit is strongly oversteer; the vehicle jack-knifes when the lead unit is oversteer and the trailing unit is understeer or slightly oversteer; the handling dynamics of the combination vehicle is stable when the leading unit is understeer.

The pneumatic tire exhibits a linear relationship between lateral force and slip angle for a given vertical load and small angles of slip. Any variations from this linear characteristic at varying vertical loads have an important impact on the handling dynamics of heavy vehicles [22]. A linear directional response is typically exhibited by vehicles for lateral accelerations of up to 0.3g. At higher levels of lateral acceleration, there is a variation in a vehicle's linear directional response and it is attributed to the non-linear relationship between slip angle and the generated lateral force at large slip angles.

For small automobiles, changes in vertical load due to cornering are relatively small [32]. Thus, there is little effect due to the sensitivity of the slip angle to lateral force relationship to changes in vertical tire load. Conversely, the nonlinearities in the handling dynamics of heavy vehicles are highly influenced by the sensitivity of the slip angle to lateral force relationship to changes in vertical load.

2.2.2 VEHICLE ROLL STABILITY

Roll stability is described as the ability of a vehicle to resist the overturning moments generated during cornering. Roll stability is influenced by the vehicle unit's track width, height of centre of mass and the kinematic and compliance properties of the suspensions.

The yaw and roll dynamics of road vehicles are coupled. For a typical road vehicle its suspension systems are designed such that the vehicle roll centre is below the centre of mass. So during steady state cornering, a road vehicle which is passively

suspended would roll outwards under the influence of the lateral accelerations acting on the vehicle units. During transient manoeuvres, the coupling between roll and yaw though the roll-yaw cross product of inertia means that yaw motions influence roll motions and vice versa.

The roll dynamics of smaller vehicles when cornering is of lesser relevance to vehicle safety than those of heavy vehicles [20]. Due to high centres of mass and narrow track widths relative to size, heavy vehicles tend to easily lose roll stability at moderate levels of lateral acceleration. Typically, the performance limit of a heavy vehicle is characterized by its loss of roll stability which means that under typical operating conditions, the maximum lateral acceleration beyond which a heavy vehicle loses its stability is limited by rollover rather than trailer swing or jack-knifing [21, 33, 34].

2.2.3 INFLUENCE OF VEHICLE DESIGN PARAMETERS

The sensitivity of yaw/roll dynamics to vehicle design parameters has been studied and reported by several authors. The yaw/roll dynamics of heavy vehicles was simulated by Fancher and Mathew [21]. Vehicle configurations considered were single unit trucks, truck/full-trailers, tractor/semi-trailers and double and triple unit long combination vehicles. Each configuration was compared on the basis of handling dynamics, high speed offtracking, low-speed offtracking, RWA ratio and roll stability. They reported that the yaw and roll stiffness and the location of the articulation joints strongly affect the interaction between the adjacent units of an articulated vehicle.

Blow *et.al.* conducted an extensive simulation study on behalf of the U.S. Department of Transportation [35]. In this study the authors considered the RWA ratio and the steady state roll stability of more than 5000 heavy vehicle configurations. It was reported that these two performance indices: RWA ratio and steady state rollover stability are most sensitive to the tire properties, vehicle mass and vehicle unit coupling design.

2.3 ADVANCED VEHICLE SUSPENSION SYSTEMS

Designing a vehicle's suspension system involves various trade-offs between ride comfort, handling dynamics, roll stability and road friendliness. Several studies have been conducted by various authors to these design trade-offs. These studies were all based on the performance limitations and constraints inherent in suspension designs [36-41].

Conventional passive suspension systems can only dissipate energy and typically consist of springs, dampers and anti-roll bars. Another class of suspension design is the *advanced suspension systems*, which in recent years has attracted significant research. Advanced suspension systems are classified into three categories; semi-active, fully active and slow active.

Semi-active suspension systems can only dissipate energy and consist of conventional springs and controllable dampers. Hardware costs for such systems are the lowest and the power consumption is limited to that required to operate the controllable damper valves [42].

Fully active suspension systems require energy to operate. In this, conventional spring and damper arrangements are replaced by powered actuators. Such systems are designed to control the motion of both the vehicle body and the wheels by operating them over a very wide frequency range [43]. Hardware costs for such systems are the highest. The bandwidth and power consumption requirement are also the most severe.

A practical compromise between the semi-active and fully active suspension systems is given by the slow active suspension systems. These systems also require energy to operate but typically consist of a passive spring and dampers in series with a low bandwidth actuator that can operate up to a maximum frequency of approximately 5 Hz. The high frequency wheel motions are controlled by the passive springs and dampers whereas the low frequency vehicle body motions (pitch and roll) are controlled by the low bandwidth actuator. The hardware costs for such systems are higher than semi-active suspension systems but lower than fully active suspension systems. The bandwidth and power consumption requirements are moderate and also lower than fully active suspension systems [44].

Karnopp conducted an in-depth feasibility study of using advanced suspension systems on road vehicles [45]. It was reported that the improvements of ride performance and vehicle's handling dynamics over a conventional passive system could be large enough to justify the additional costs and system complexity.

Most advanced suspension systems are developed for small single unit passenger vehicles [46-50]. These systems provide good ride, handling dynamics and

roll stability. Lotus and Cranfield Institute of Technology developed a fully active suspension system to be used in Formula 1 (*F1*) racing [51, 52]. Track tests of the developed system showed that it was able to maintain constant suspension travel and altitude during acceleration, braking and cornering.

Glasner *et.al.* [53] considered the use of advanced suspension systems in heavy vehicles. It was reported that the use of semi-active and slow active suspension systems was feasible, but the use of fully active suspension systems was not feasible to significantly improve the heavy vehicle's handling dynamics that could justify the high hardware and operating costs.

2.4 VEHICLE ROLLOVER PREVENTION

Over the last two decades many vehicle rollover prevention systems have been investigated by researchers. These systems can be broadly classified into four categories based on the incorporated actuation mechanism, namely, active stabilizer, active wheel steering, differential braking and active suspension.

Furleigh *et.al.* [54] proposed to enhance the roll stability of an AHV by using multiple steerable axles. The presented controller assumed that the steer angle of the lead unit's rear axle is proportional to front axle's steer angle and this proportionality changes with vehicle forward speed. Both low-speed manoeuvrability and high-speed performance simulations were conducted. It was reported that during a high-speed obstacle avoidance manoeuvre, the lateral acceleration at the trailing unit could be reduced by steering the lead unit's rear axle.

Cheng [55] presented an investigation to enhance the rollover stability and safety of AHVs at high speeds and improve the manoeuvreability while reducing tire and road wear at low speeds. His research considered the use of active trailer steering. Two controllers were developed: PID controller for low speeds and LQR controller for high speeds. The controlled vehicle was reported to have narrow swept path width, low lateral tire forces, low high-speed and transient off-tracking while reducing RWA ratio by almost 25%.

Carlson and Gerdes [56] developed a controller with differential braking and front steer-by-wire for a vehicle. The control strategy was developed using the Model Predictive Control (MPC) theory. It was reported that the developed controller could effectively reduce the peak roll angle of the vehicle while simultaneously tracking the yaw rate command given by the driver. The authors noted that the computational complexity of the MPC-based controller increased rapidly with state variable dimensions.

Palkovics *et.al.* [19, 57] proposed an electronic braking system to improve the roll stability of a single unit truck. They reprogrammed an existing electronic braking system such that it regularly applied to each wheel a small braking force and monitored the slip response of the vehicle. This proposed system benefitted with low power consumption and zero additional hardware cost. This system effectively changed the vehicle path with the trade-off that the directional controllability of the vehicle was reduced in emergency situations.

Lewis and El-Gindy [58] investigated rollover prevention strategies for a truck/semi-trailer combination based on a sliding mode controller and differential braking. It was reported that the torque generated by differential braking could be effective in preventing rollover of the AHV.

Two control systems were compared by Gaspar *et.al.* [59] for the rollover prevention of heavy vehicles, namely, active braking mechanism and active anti-roll bars. The active braking system is activated only when the vehicle comes close to rollover which is determined by normalized load transfer. Meanwhile the active anti-roll bars are used to generate a stabilizing moment to balance the destabilizing moment at all times. It was reported that the path of the vehicle was drastically changed from the desired path by the effects of the brake moment. This disadvantage of the active braking system constantly impelled the driver to intervene so as to counteract the influence of braking on the yaw motion of the vehicle.

An active roll control system comprising of a hydraulic 5^{th} wheel and an active suspension was proposed by Dunwoody and Froese [60] to control the roll motion of the vehicle. This proposed active roll control system was reported to increase the vehicle's static rollover threshold by approximately 30%.

Lin *et.al.* [61-63] proposed a roll control system for single unit and articulated heavy vehicles based on active suspension and lateral acceleration feedback. Low frequency steering inputs needed to follow the road geometry were considered to derive the steering input spectrum along with higher frequency inputs needed to

successfully complete a lane change manoeuvre. It was reported that the static rollover threshold of a single unit truck with active suspension was improved by 66% and the total *root of mean square* (RMS) load transfer in response to a typical random steering input was reduced by 34%.

Sampson [64] presented an in-depth study of LCVs and LQR based method for designing a partial state feedback controller using active anti-roll bars. It was reported that the designed system could enhance steady state rollover stability of a rigid single unit vehicle by 23% and a torsionally rigid tractor semi-trailer combination by as much as 30%.

Miege [65] presented an investigation of an experimental tractor/semi-trailer combination and PID control theory to develop a controller using hydraulic actuators and anti-roll bars. This control strategy was validated with the test data but was found to be very slow. An optimal control strategy was also proposed to equalize the lateral load transfer between all controlled axles which provided maximum inward roll. It was reported that the proposed optimal control strategy could reduce the peak normalized load transfer by as much as 20% in comparison to a passive vehicle.

2.5 HIGH-SPEED AND LOW-SPEED PERFORMANCE TRADE-OFF

Researchers have investigated several ways to improve the trade-off between high speed RWA and low speed PFOT. Aurell and Edlund [66] reported that the type of steering mechanism used and the location of the steered axles have a substantial effect on the dynamic stability of an AHV. Researchers have investigated systems that

use passive steering systems at low speeds, decreasing low speed PFOT value and active steering systems at medium to high speeds thereby improving stability at high speeds [5, 67, 68]. El-Gindy *et.al.* [5] designed active yaw controllers for a tractor/full-trailer combination using RWA ratio as a control criterion. Rangavajhula and Tsao [68, 69] have implemented LQR controller for active trailer steering systems of AHVs to improve the compatibility between high speed RWA and low speed PFOT. Islam *et.al.* [70-73] also developed active trailer steering systems using LQR technique. The authors further proposed novel approaches to the design synthesis of such systems but were limited by the simplicity of their vehicle model used.

2.6 VEHICLE DYNAMICS OF COMPUTER SIMULATION

Researchers have been using mathematical models for many years to simulate vehicle dynamics and control systems [74].There are several advantages of using computer simulations; the ability to study the behavior of existing systems, the possibility of evaluating alternate designs prior to building prototypes, the scope of studying the response of hardware components and the behavior of human drivers through *hardware-in –the-loop* or *driver-in-the-loop* real-time simulations, respectively [75].

There exist many multibody system simulation programs, such as TruckSim, ADAMS and DADS [55, 75, 76] which can reliably generate complex non-linear vehicles models with many degrees of freedom. These programs perform well for passive vehicle models, but their complexities are impractical to design any vehicle

control system. It is thus preferred to develop simple vehicle models to design vehicle control systems. Such models should judiciously include all necessary vehicle states while neglecting all the irrelevant ones. Previous studies have shown that well designed control systems based on simplified vehicle models often perform quite well [77-79].

2.7 RESEARCH OBJECTIVES

The main objectives of this thesis are as follows:

1) To develop a vehicle model that is capable of representing the roll of an AHV within reasonable approximations. To design an *active roll stability control (ARSC)* system based on the developed vehicle model.
2) To investigate a design synthesis method for passive vehicle systems to achieve optimal vehicle parameters in order to simultaneously improve the high-speed and low-speed directional performance of an AHV.

CHAPTER 3

DESIGN AND SIMULATION TOOLS

3.1 INTRODUCTION

This chapter describes the design and simulation tools used to perform the design synthesis of AHVs. The fundamental numerical optimization is outlined with an emphasis on one particular global search algorithm along with the basic control theory used in this research. Various performance indices and test manoeuvres for AHVs are also introduced.

3.2 METAHEURISTIC OPTIMIZATION

In a general sense, optimization is defined as follows [80],

"An act, process, or methodology of making something (as a design, system, or decision) as fully perfect, functional, or effective as possible; ***specifically***: the mathematical procedures (as finding the maximum of a function) involved in this".

Many real-world optimization problems in science and engineering are complex and often difficult to solve in an analytical manner within reasonable amount of time. A good way to tackle such problems is using approximate algorithms. Metaheuristic optimization represents a family of approximate optimization techniques [81]. Metaheuristic robust algorithms can be available which are highly flexible and simple

to implement. These algorithms help solving large real-world problems and providing acceptable solutions faster.

The word *heuristic* comes from the Greek work *heuriskein*, which means the art of discovering new schemes to solve problems. The suffix *meta* is also a Greek work and means, upper level methodology. F. Glover (1986) first introduced the term *metaheuristic* in his paper [82].

3.3 GENETIC ALGORITHM

Genetic Algorithm (GA) is a population-based metaheuristic search method. GA is an adaptive heuristic search algorithm premised on the evolutionary ideas of natural selection and genetic (survival of the fittest). The idea of GA can be traced back to 1950s, but the project done by John Holland [83] at University of Michigan led to GA, as it is presented today. Basically, the algorithm represents a search strategy inspired by the natural selection mechanics and reproduction in natal systems. The strategy is based on the process of natural selection in which the more capable offsprings survive and the rest die. Moreover, GA is a branch of evolutionary algorithms which are derived from evidence that was originally observed and documented by Charles Darwin. The concept of "survival of the fittest" has been taken, implemented, and developed for designing the GA in which natural evolution and adaptation to environment variation is simulated mathematically.

Due to the fact that GA can proceed with a large population of designs, the algorithm has the merit of tackling the globally optimal solution [84]. Basically, GA

starts from an initial set, or first generation, of randomly chosen designs with uniform probability distribution and continues with selecting the fittest individuals, 'survival of the fittest', which is known as selection. The next step would be regeneration, at which the algorithm takes advantage of two mathematical methods, crossover and mutation, to generate new offsprings by the selected parents from the previous generation. Moreover, another advantage of GA is that for running the algorithm, i.e. initializing the population, selection, regeneration, no gradient information is required; only evaluation of the objective function and the constraints are necessary to determine the fitness value. Such an advantage makes GA flexible and gives it the ability to deal with problems having a complex objective function, where derivative is difficult to obtain or unachievable. On the other hand, the random nature of GA gives it the ability of escaping the local optima.

Due to the above discussed capabilities, recent years have witnessed an exponential growth in the implementation of GA in a vast spectrum of science and engineering fields. Forrest [85] collected a good summary of GA applications in science and engineering problems up to 1993.

In summary, some comments on GA are as follows.

- GA works on function estimates only and does not require function derivatives.
- GA proceeds from several points in the landscape (population); hence, the method has a better probability of finding the global optima.

- GA allows that the design variable spaces could be a mix of continuous and discrete variables.
- GA uses probabilistic transition rules, not deterministic rules.
- GA can be implemented using parallel CPUs.

GA is a global search algorithm which requires evaluating the objective function only, not the function derivatives. It has been utilized for solving a vast range of numerical simulation problems. In this thesis, one of the objective functions comes from a set of highly non-linear and complicated equations, which makes using classic optimization methods impossible. GA has been implemented to tackle such a problem.

3.3.1 GENOME

In GA, each objective has a set of potential solutions. This set of potential solutions is defined as a population and each solution of this population is termed as an individual. The encoding of an objective's potential solution denoted by an individual is called as its *genome*. In a given population, many individuals may have similar or same genome. A genome is sometimes referred to as a *chromosome* which comprises of many units of genetic information as is also true in nature. Each of these single units of genetic information is termed as a *gene* and further consists of one or more possibilities called *alleles*, as shown in figure 3.1. In GA, the number of genes in a genome is fixed.

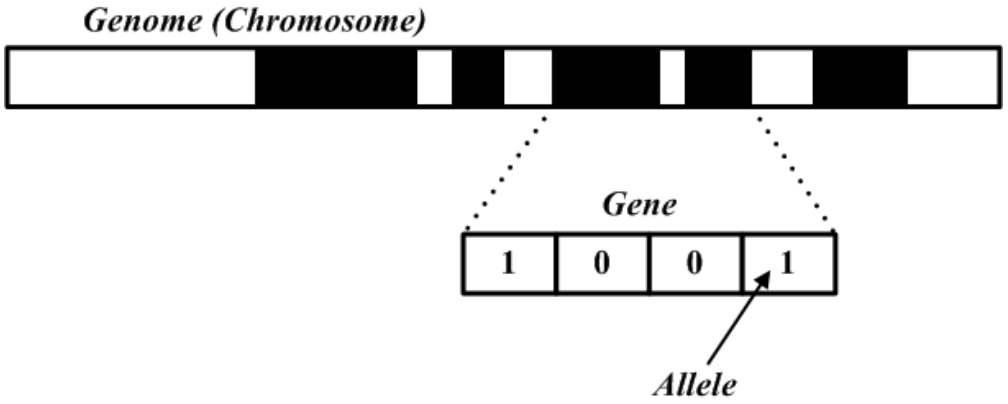

Figure 3.1: Genome representation

3.3.2 FITNESS FUNCTION

The *fitness function* in GA determines the goodness or fitness of a solution where the parameter is a genome. Fitness function is also referred as the *objective function* and its choice of selection is very critical for the GA to reach the global optima for a given problem.

3.3.3 GA OPERATORS

Genetic algorithm like all other evolutionary algorithms works based on nature's three vital forces of natural selection, mating and mutation. These in GA correspond to selection, crossover and mutation respectively and are referred as genetic operators. All genetic operators work on genes, individuals and populations alike.

3.3.3.1 SELECTION

The individuals chosen for mating are determined by the selection operator. Choosing a selection method which each time picks only the best individuals will

make the population quickly converge to that individual. Hence, the selection operator should be such, which though biased towards better individuals; it also selects some that are not all that good. This approach helps prevent premature convergence and a loss of diversity [81]. Some of the common selection methods are: roulette wheel selection, in which the likeliness of choosing an individual is proportional to the individual's score; tournament selection, in which a number of individuals are chosen using roulette wheel selection and the best of these are selected for mating; rank based selection, in which the best individual is chosen each time.

3.3.3.2 CROSSOVER

Crossover is the mating of individuals and refers to the process of *genetic recombination*. In this process, the genome of a child is formed by randomly combining the genes of two parents. The simplest way to perform crossover is by selecting a random gene along the length of the genome and then swap all the genes after that point, as shown in figure 3.2.

Figure 3.2: Crossover operation

3.3.3.3 MUTATION

Mutation operation generates a completely new and random genome. It operates by randomly choosing a chromosome's gene and then changing its one or more alleles, as shown in figure 3.3. The main role of this operator is to introduce a certain amount of randomness to the search. This in turn helps increase the probability of finding the global optima.

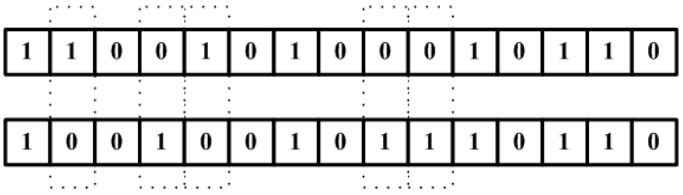

Figure 3.3: Mutation operation

3.4 LINEAR QUADRATIC REGULATOR

Kalman introduced the Linear Quadratic Regulator (LQR) technique [86, 87]. The infinite horizon, continuous time LQR problem considers the linear time-invariant plant and the system is described as:

$$\dot{x} = Ax + Bu \tag{3.1}$$

The time-invariant quadratic cost function is given by:

$$J = \int_0^\infty (x^T Q x + u^T R u) dt \tag{3.2}$$

In equation (3.1) $A \epsilon \mathbb{R}^{nxn}$ is the state matrix, $B \epsilon \mathbb{R}^{nxm}$ is the input matrix, $x \epsilon \mathbb{R}^{nx1}$ is the state vector and $u \epsilon \mathbb{R}^{mx1}$ is the control vector. In equation (3.2) $Q = Q^T \geq 0$ and $R = R^T > 0$ where Q and R are the weighting matrices.

The feedback control law that minimizes the time-invariant quadratic cost function is given as:

$$u = -Kx \tag{3.3}$$

where K is the control gain matrix defined by:

$$K = R^{-1}B^T S \tag{3.4}$$

provided

$$A^T S + SA - SBR^{-1}B^T S + Q = 0 \tag{3.5}$$

Equation (3.5) is known as the Algebraic Riccati Equation (ARE) and is used for calculating S required in equation (3.4). Further details on LQR theory can be found in references [88] and [89].

3.5 TEST MANOEUVRES EMULATED

Two types of dynamic simulations have been used in this thesis, namely open-loop simulation (chapter 4) and closed-loop simulations (chapter 5).

3.5.1 OPEN-LOOP DYNAMIC SIMULATION

The open-loop dynamic simulation approach requires precise application of a predetermined steer sequence. In this thesis, to assess the dynamic behavior of AHVs, one-period sinusoidal steer input [66, 68, 69, 90] has been used. A single lane change manoeuvre is simulated such that the vehicle is travelling at a constant speed of 88 km/h along a straight path and a sudden lane change occurs. The lateral displacement of the AHV in the lane change is 1.46 m. For this open-loop dynamic simulation, the steering input (in radians) takes a single sinusoidal wave as:

$$\delta(t) = A sin(\frac{2\pi}{T} t) \tag{3.6}$$

where the period T is 2.5 seconds [91, 92] and the value of amplitude A is selected such that the vehicle is able to complete the single lane change manoeuvre [93]. Figure 3.4 shows the steering input used in this thesis during any open-loop dynamic simulation.

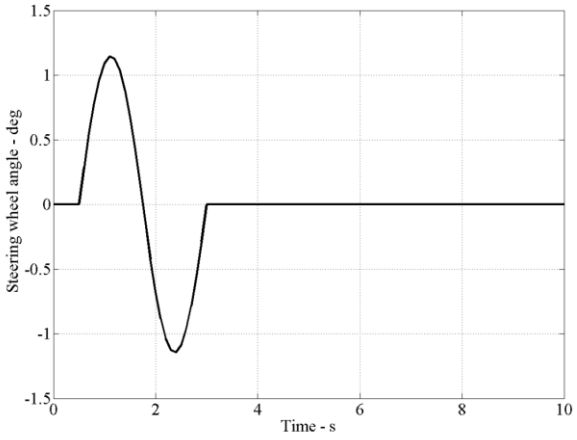

Figure 3.4: Steering angle input of single lane change manoeuvre

3.5.2 CLOSED-LOOP DYNAMIC SIMULATIONS

The closed-loop dynamic simulations are defined in the TruckSim software package (described in chapter 5). These simulations are closed-loop steer control processes. A driver model is introduced which enables the AHV to follow a well-defined path. Two simulations are defined; one for determining the high-speed rearward amplification (RWA) ratio and the second for determining the low-speed path following off-tacking (PFOT).

Safety and cost concerns make it impractical to perform field testing of concept designs for its validation and assessing its performance. A more practical solution to this is to use computer simulations based on well defined models. In these closed-loop tests, a desired vehicle trajectory is achieved by continuously monitoring the vehicle response and adjusting the steering input accordingly. In such simulations, the driver is assumed an integral part of the system, such that the mathematical model of the whole system involves a driver model [94]. Furthermore, such computer simulations provide a safe and cost effective way to assess the interactions between the human driver and the vehicle. This approach is efficient and effective even before a single vehicle or its subsystems are produced for field tests.

3.5.2.1 HIGH-SPEED TESTING MANOEUVRE EMULATED

The high-speed testing manoeuvre is used to assess the high-speed RWA ratio of AHVs. The testing manoeuvre simulated is based on the high-speed single lane change manoeuvre defined in SAE J2179 testing procedure [92]. In this manoeuvre,

the vehicle forward speed is kept constant at a speed of 88 km/h while it is laterally displaced a distance of 1.46 m. Figure 3.5 shows the schematics of this manoeuvre.

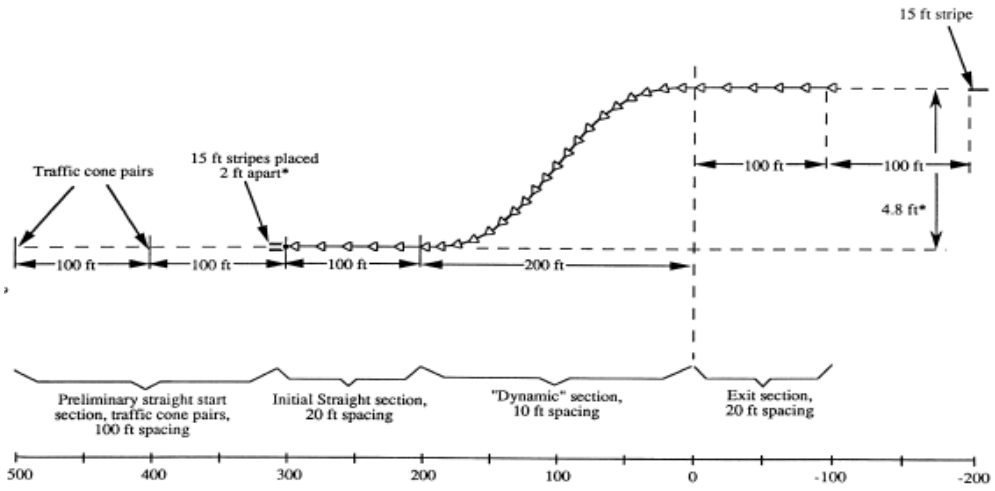

Figure 3.5: Schematics of high-speed single lane change manoeuvre specified in SAE J2179 testing procedure [92]

3.5.2.2 LOW-SPEED TESTING MANOEUVRE EMULATED

The low-speed testing manoeuvre is used to assess the low-speed PFOT value of AHVs. In the testing manoeuvre emulated the vehicle is manipulated to complete a 90^0 intersection turn [94], in which the curved path has a radius of 12.5 m. The vehicle forward speed is kept constant at 5 km/h. The maximum swept path width is calculated by taking the difference between the path followed by the centre point of the vehicle's foremost axle and the path followed by the centre point of the vehicle's rearmost axle. Figure 3.6 shows the profile of the pre-defined path for the simulation.

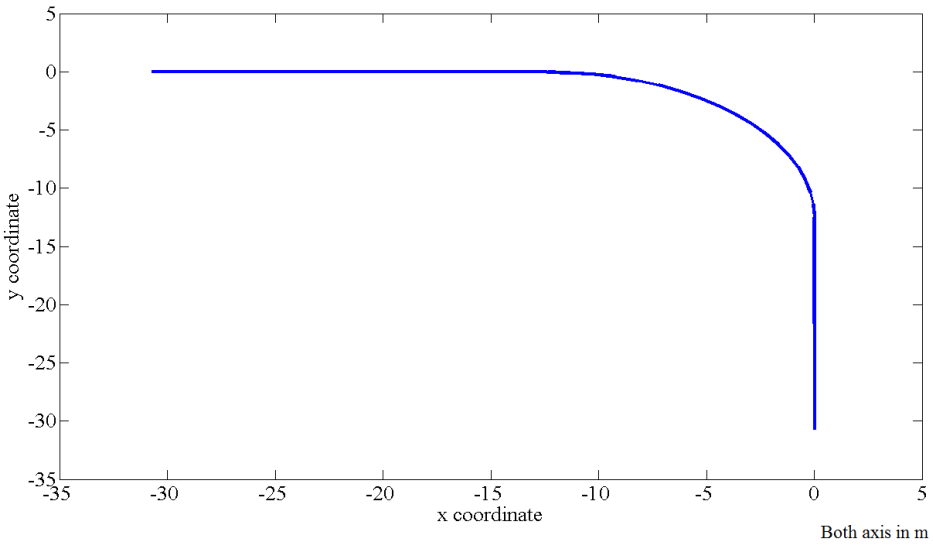

Figure 3.6: Pre-defined path for low-speed testing manoeuvre emulated

CHAPTER 4

ACTIVE ROLL STABILITY CONTROL SYSTEMS FOR AHVs

4.1 INTRODUCTION

This thesis presents the investigation on active roll stability control for AHVs during high speed manoeuvres. A 3-dimensional (3-D) linear yaw/roll model with 5 degrees of freedom (DOF) is developed. Based on this model a linear quadratic regulator (LQR) controller is developed to enhance the roll stability of a tractor/semi-trailer combination.

4.2 VEHICLE SYSTEM MODELING

The use of a simplified vehicle model reduces computational expense of the control system, but may lead to low fidelity. On the other hand, a sophisticated vehicle model can increase the accuracy of the control system, but it will increase its computational cost. Hence, a 3-D yaw/roll model with 5-DOF is developed. This model embodies the most important dynamic features of an AHV's handling.

4.2.1 ASSUMPTIONS

Assumptions are made in deriving the vehicle model. These assumptions are listed as follows:

- Each vehicle unit is considered as a rigid body

- Axles of each vehicle unit are considered as a single, mass less rigid body having roll motion
- The vehicle units have no pitch or bounce motion
- All effects of road inputs (bumps, dips, cross gradients) are neglected
- All effects of aerodynamic inputs are neglected
- Effects of vehicle tractive thrust are neglected i.e. the tractive thrust is considered to be evenly distributed between driving wheels and that it doesn't contribute to vehicle yaw motion
- Tire properties are linearized. The effects of camber thrust, roll steer and aligning moment are neglected
- The suspension roll stiffness and damping coefficients are constant in the range of roll motion involved
- No braking forces applied on any of the wheels
- All wheels on an axle have the same slip angle and are modeled as a single wheel in accordance to the *Bicycle* model
- Cornering stiffness of the three semi-trailer axles are the same
- The angular displacements and the articulation angle between the two vehicle units is small during manoeuvres.
- The vehicle forward speed is constant during manoeuvres.

4.2.2 ANTI-ROLL BAR MECHANISM

A schematic sketch of an anti-roll bar installed on a vehicle is shown in figure 4.1 (a). Points A and B are attached to the chassis and points C and D are attached to

the axle. Whenever the vehicle rolls, a force F develops at each of these points. The forces acting at points A and B generate a roll moment *M* about the roll axis of the vehicle. On the other hand, the forces acting at points C and D cause a torque *T* in the section AB of the anti-roll bar.

The torque *T* which is exerted on the anti-roll bar equals *Fw* which results in a roll moment *M* on the vehicle equaling *F2d*. Hence, the relationship between the roll moment *M* and the torque *T* is given by:

$$M = \frac{2d}{w} T \tag{4.1}$$

The torque T equals to $k\Phi'$, where *k* represents torsional stiffness and Φ' denotes the twist angle of the anti-roll bar. The relationship between the vehicle roll moment *M* and the twist angle of the anti-roll bar is given by:

$$M = \frac{2d}{w} k\Phi' \tag{4.2}$$

Due to the roll of the sprung mass, point B moves to point B', a distance y relative to A, as shown in figure 4.1 (a). With this action, the relative roll angle Φ_r between the unsprung mass and the sprung mass is *y/2d* and the twist angle of the anti-roll bar Φ' is *y/w*, as shown in figure 4.1 (b).

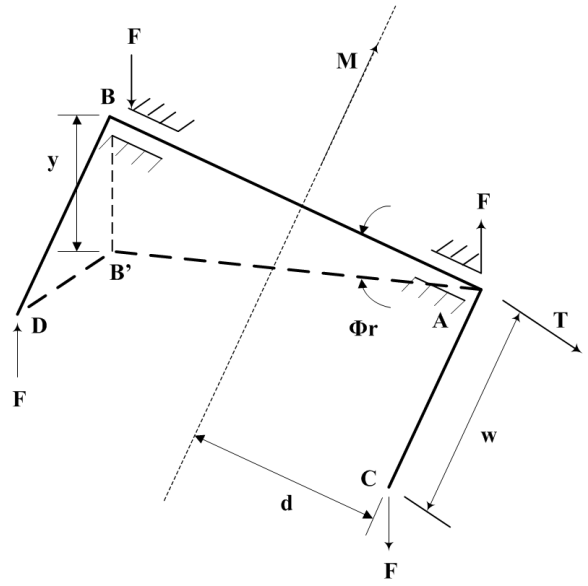

(a)

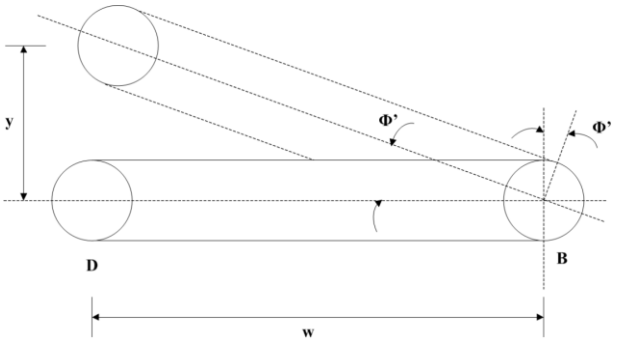

(b)

Figure 4.1: Geometry of anti-roll bar

The relationship between the relative roll angle Φ_r and the twist angle of the anti-roll bar Φ' is given by:

$$\Phi' = \frac{2d}{w}\Phi_r \tag{4.3}$$

Substituting equation (4.3) into equation (4.2) gives:

$$T = K_{ac}\Phi_r \tag{4.4}$$

where K_{ac} is the roll stiffness of the anti-roll bar and equals $k(\frac{2d}{w})^2$.

The linear analogy of the roll suspension studied in the research is shown in figure 4.2. For accurate prediction of roll angle, the tire vertical stiffness is considered. An active suspension consisting of an actuator (marked *A*) is introduced in series with the passive anti-roll bar (marked K_{ac}). The roll angles generated by the anti-roll bar and the actuator are represented as Φ_1 and Φ_2 respectively. The relative roll angle of the unsprung mass (due to tires) with respect to the sprung mass is represented by Φ_3, and Φ_t is the roll angle of the unsprung mass. The total suspension roll moment is given by:

$$M_s = L\left(\dot{\Phi} - \dot{\Phi}_t\right) + K(\Phi - \Phi_t) - T_{actuator} \tag{4.5}$$

where *L* and *K* are the roll damping and the roll stiffness of the shock absorbers (dampers) and springs, respectively. The actuator force is defined positive in tension. $T_{actuator}$ is the torque generated by the actuator and it equals to $K_{ac}\Phi_1$. The suspension roll moment M_s equals to the roll moment developed by the tires M_t, such that $M_s = M_t = K_t\Phi_t$ and K_t represents the roll stiffness of the tires. Hence, equation (4.5) becomes:

$$K_t\Phi_t = L\left(\dot{\Phi} - \dot{\Phi}_t\right) + K(\Phi - \Phi_t) - T_{actuator} \tag{4.6}$$

Rearranging equation (4.6) leads to:

$$L\left(\dot{\Phi} - \dot{\Phi}_t\right) + K(\Phi - \Phi_t) - (K_t\Phi_t) - T_{actuator} = 0 \tag{4.7}$$

The active anti-roll bar and tire flexibility are augmented to the system equations using equation (4.7).

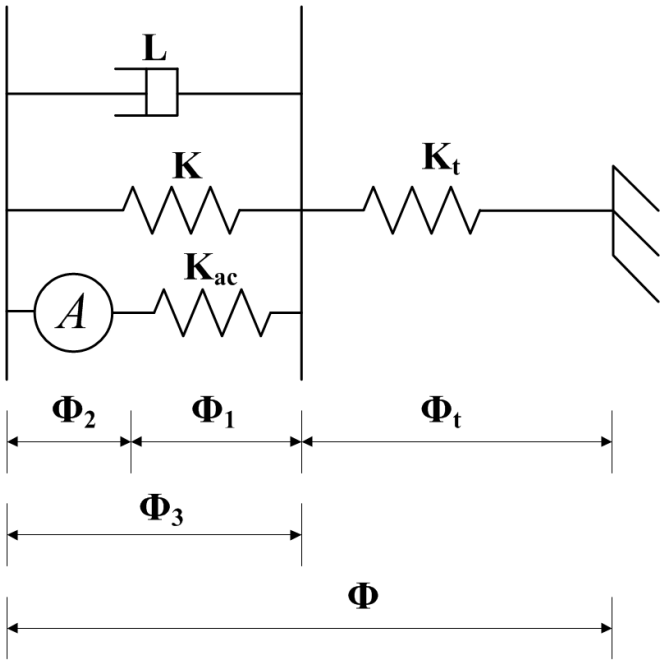

Figure 4.2: Linear analogy of the roll suspension

4.2.3 YAW/ROLL VEHICLE MODEL

To generate the yaw/roll vehicle model, two types of coordinate systems are defined; the global coordinate system and the body-fixed coordinate system.

The global coordinate system (X, Y, Z) is defined as a right handed orthogonal axis system whose z-axis points up and is parallel to the gravity vector. The origin of the Z-axis could be any point on the ground plane.

The body-fixed coordinate systems (x_i, y_i, z_i), i = 1, 2, 1 for the tractor and 2 for the semi-trailer are also defined as right handed orthogonal systems. The z-axis points up and it parallel to the gravity vector. The x-axis points forward and is parallel to the ground. The roll axis is assumed to be horizontal and parallel to the ground and on the same plane as the x-axis. The y-axis is perpendicular to both the x-axis and the z-axis

points left of the vehicle unit whose origin is a point on the roll axis, directly below the centre of gravity (CG) of the vehicle unit. The rear view of the semi-trailer is shown in figure 4.3. The top view and the side view of the tractor/semi-trailer combination are shown in figures 4.4 and 4.5 respectively.

The five degrees of freedom of the vehicle model are; lateral, yaw and roll motions of the tractor and the yaw and roll motions of the semi-trailer.

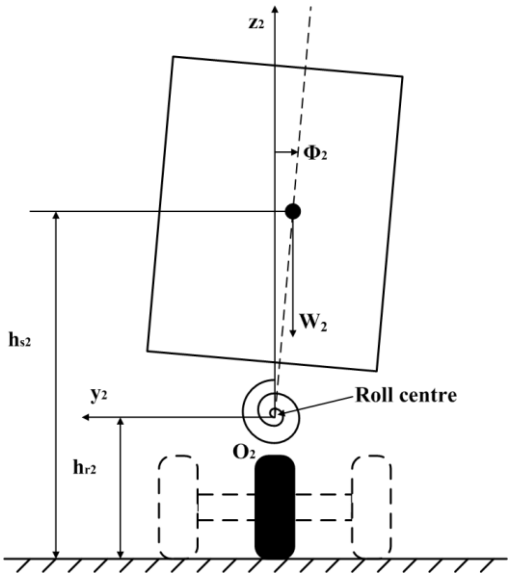

Figure 4.3: Rear view of semi-trailer

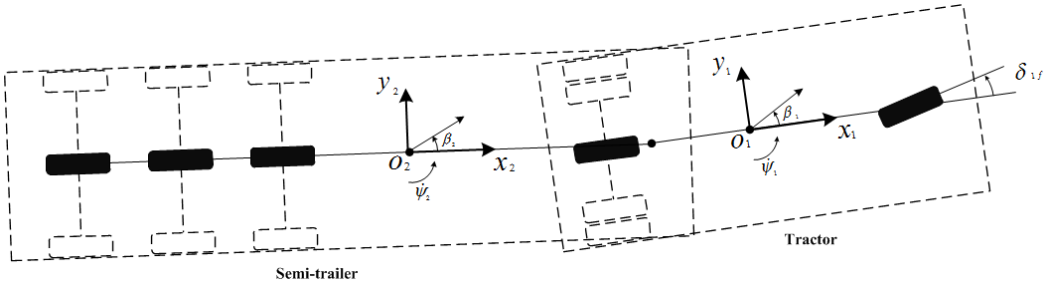

Figure 4.4: Top view of tractor/semi-trailer

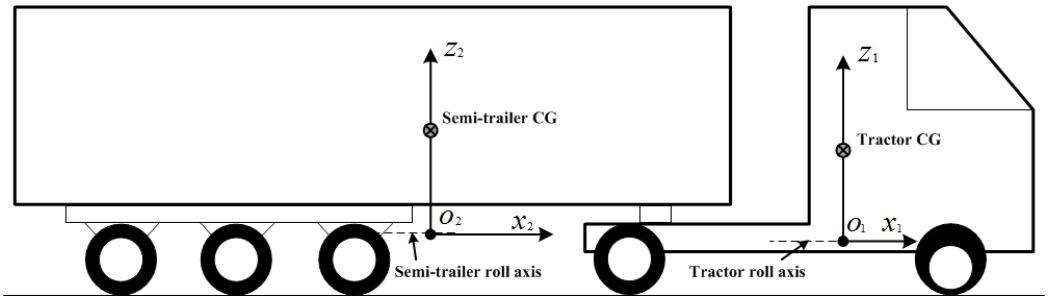

Figure 4.5: Side view of tractor/semi-trailer

The equations representing the tractor's motion are given as:

$$m_1u_1(\dot{\beta}_1 + \dot{\Psi}_1) - m_{s1}(h_{s1} - h_{r1})(\ddot{\Phi}_1) = Y_{\beta 1}\beta_1 + Y_{r1}(\dot{\Psi}_1) + Y_{\delta 1f}\delta_{f1} + F_{y1} \tag{4.8}$$

$$-I_{xz1}(\ddot{\Phi}_1) + I_{zz1}(\ddot{\Psi}_1) = N_{\beta 1}\beta_1 + N_{r1}(\dot{\Psi}_1) + N_{\delta 1f}\delta_{f1} + l_{c1}F_{y1} \tag{4.9}$$

$$(I_{xx1} + m_{s1}(h_{s1} - h_{r1})^2)(\ddot{\Phi}_1) - I_{xz1}(\ddot{\Psi}_1) = m_{s1}g(h_{s1} - h_{r1})\Phi_1 + m_{s1}u_1(h_{s1} - h_{r1})(\dot{\beta}_1 + \dot{\Psi}_1) - m_{s1}(h_{s1} - h_{r1})^2(\ddot{\Phi}_1) - (K_{f1} + K_{r1})(\Phi_1 - \Phi_{t1}) - (L_{f1} + L_{r1})(\dot{\Phi}_1 - \dot{\Phi}_{t1}) + K_{12}(\Phi_2 - \Phi_1) - F_{y1}h_{cr1} + u_{c1} \tag{4.10}$$

$$(L_{f1} + L_{r1})(\dot{\Phi}_1 - \dot{\Phi}_{t1}) + (K_{f1} + K_{r1})(\Phi_1 - \Phi_{t1}) - (K_{tf1} + K_{tr1})(\Phi_{t1}) - u_{c1} = 0 \tag{4.11}$$

The equations representing the semi-trailer's motion are given as:

$$m_2u_2(\dot{\beta}_2 + \dot{\Psi}_2) - m_{s2}(h_{s2} - h_{r2})(\ddot{\Phi}_2) = Y_{\beta 2}\beta_2 + Y_{r2}(\dot{\Psi}_2) - F_{y1} \tag{4.12}$$

$$-I_{xz2}(\ddot{\Phi}_2) + I_{zz2}(\ddot{\Psi}_2) = N_{\beta 2}\beta_2 + N_{r2}(\dot{\Psi}_2) - l_{c2}F_{y1} \tag{4.13}$$

$$(I_{xx2} + m_{s2}(h_{s2} - h_{r2})^2)\left(\ddot{\Phi}_2\right) - I_{xz2}\left(\ddot{\Psi}_2\right) = m_{s2}g(h_{s2} - h_{r2})\Phi_2 +$$

$$m_{s2}u_2(h_{s2} - h_{r2})\left(\dot{\beta}_2 + \dot{\Psi}_2\right) - m_{s2}(h_{s2} - h_{r2})^2\left(\ddot{\Phi}_2\right) - K_{r2}(\Phi_2 - \Phi_{t2}) -$$

$$L_{r2}\left(\dot{\Phi}_2 - \dot{\Phi}_{t2}\right) - K_{12}(\Phi_2 - \Phi_1) + F_{y1}h_{cr2} + u_{c2} \quad (4.14)$$

$$L_{r2}\left(\dot{\Phi}_2 - \dot{\Phi}_{t2}\right) + K_{r2}(\Phi_2 - \Phi_{t2}) - K_{tr2}(\Phi_{t2}) - u_{c2} = 0 \quad (4.15)$$

Equations (4.8) and (4.12) represent the lateral motion of the tractor and semi-trailer respectively. Equations (4.9) and (4.13) denote the yaw moment of the tractor and semi-trailer, respectively. Equations (4.10) and (4.14) express the roll moment of the tractor and semi-trailer, respectively. Equations (4.11) and (4.15) determine the axle roll moment of the tractor and semi-trailer, respectively.

The kinematic constraint equation between the tractor and the semi-trailer is cast as:

$$\left(-\frac{h_{c1}}{u_1} + \frac{h_{r1}}{u_1}\right)\left(\ddot{\Phi}_1\right) + \left(\frac{h_{c2}}{u_2} - \frac{h_{r2}}{u_2}\right)\left(\ddot{\Phi}_2\right) + \dot{\beta}_1 - \dot{\beta}_2 - \frac{l_{c1}(\ddot{\Psi}_1)}{u_1} - \frac{l_{c2}(\ddot{\Psi}_2)}{u_2} + \dot{\Psi}_1 -$$

$$\dot{\Psi}_2(t) = 0 \quad (4.16)$$

The notations are given in nomenclature. The detailed derivations of equations (4.8)-(4.16) can be referred in [27, 55, 64, 95]. These equations can be expressed in the state-space form as:

$$\dot{x} = Ax + Bu + C\delta \quad (4.17)$$

where the matrices A, B and C are provided in Appendix A and δ is the steering input. The state vector x is expressed as:

$$x = [\Phi_1\ \dot{\Phi}_1\ \beta_1\ r_1\ \Phi_2\ \dot{\Phi}_2\ \beta_2\ r_2\ \Phi_{t1}\ \Phi_{t2}]^T \quad (4.18)$$

and the control vector u is expressed as:

$$u = [\mathrm{u}_{c1}\ u_{c2}]^T \tag{4.19}$$

Note that *u* is the control vector related to the force generated by the actuators of the active anti-roll bar. The elements u_{c1} and u_{c2} are the generated actuator forces of the tractor and the semi-trailer active anti-roll bars, respectively.

4.3 LQR CONTROLLER DESIGN

The design for the active roll stability control (ARSC) system is based on the linear quadratic regulator (LQR) technique. The design criterion is to minimize the roll angles of the tractor and semi-trailer sprung masses and also the roll angles of the tractor and semi-trailer axles. The LQR controller design is hence an optimization problem so as to minimize the cost function:

$$J = \int_0^\infty (q_1\Phi_1^2 + q_2\dot{\Phi}_1^2 + q_3\beta_1^2 + q_4\mathrm{r}_1^2 + + q_5\Phi_2^2 + q_6\dot{\Phi}_2^2 + q_7\beta_2^2 + \\ + q_8\mathrm{r}_2^2 + q_9\Phi_{t1}^2 + q_{10}\Phi_{t2}^2 + + r_{c1}\mathrm{u}_{c1}^2 + r_{c2}u_{c2}^2)dt \tag{4.20}$$

subject to equation (4.17). The control vector *u* obtained by solving the Algebraic Riccati Equation is the solution of the optimization problem and takes the form:

$$u = -Kx \tag{4.21}$$

where *K* is the control gain matrix with a dimension of 2x10, x is the state variable vector defined by equation (4.18) and u is the control variable vector defined by equation (4.19). In equation (4.20), q_1, q_2, q_3, q_4, q_5, q_6, q_7, q_8, q_9 and q_{10} are elements of the weight matrix Q and r_1 and r_2 are the elements of the weight matrix R

(Appendix A). The weighting factors of weight matrix Q impose penalties upon the magnitude and durations of the variables of the state vector. The last two terms on the right side of equation (4.20) represents the total energy consumption of the ARSC system. The elements of matrices *Q* and *R* are determined by the trial and error approach and are given in Appendix A.

4.4 SIMULATION AND RESULTS

4.4.1 MODEL VALIDATION

The vehicle model described in section 4.2 is validated in two stages, i.e. eigenvalue analysis and comparison with TruckSim model.

With the given vehicle system parameters listed in Appendix B, eigenvalue analysis of the system matrix *A* shown in equation (17) can be conducted. The eigenvalue analysis reveals that all eigen vectors have negative real parts as shown in table 4.1. Stable motion modes are represented by the presence of negative real parts of the eigen vectors of the system matrix *A*. Eigenvalue analysis is a good indicator of vehicle stability, but is at the same time a vague way of validating a vehicle model.

After the eigenvalue analysis, the 5-DOF linear yaw/roll model is compared against the model from the multibody vehicle dynamics software TruckSim (further information about TruckSim will be provided in chapter 5).

For the purpose of comparison, the two models are defined with the same geometrical parameters. The test procedure simulated is as described in section 3.5.1.

Table 4.1: Eigenvalue analysis

Root	Real Part	Imaginary Part
1	-6.5763	0
2	-8.6979	0
3	-0.0194	+0.1527i
4	-0.0194	-0.1527i
5	-0.0386	+0.0342i
6	-0.0386	-0.0342i
7	-0.0060	+0.0342i
8	-0.0060	-0.0342i
9	-0.0137	+0.0318i
10	-0.0137	-0.0318i

The dynamic performance of the two models is compared. The tractor and semi-trailer side slip angles can be compared for the two models as shown in figure 4.4 and 4.5, respectively. The tractor and semi-trailer side slip time histories for the two models agree well for the dynamic manoeuvre.

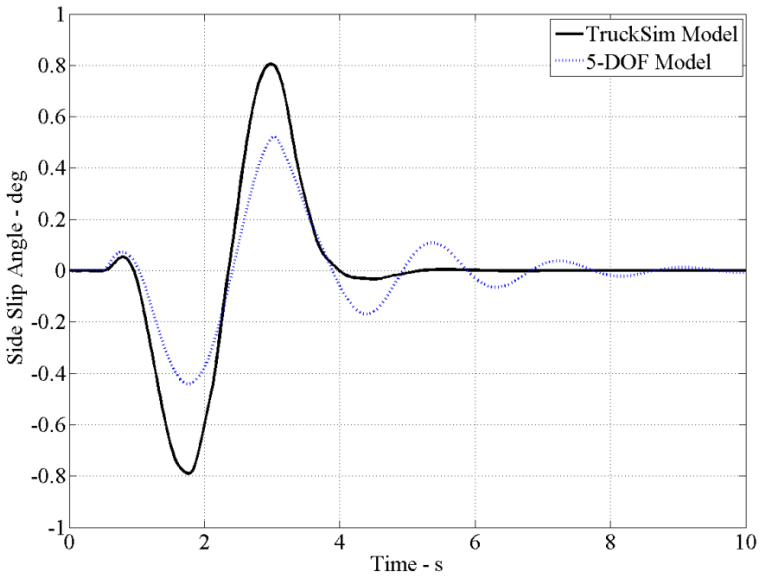

Figure 4.4: Tractor side slip angle versus time

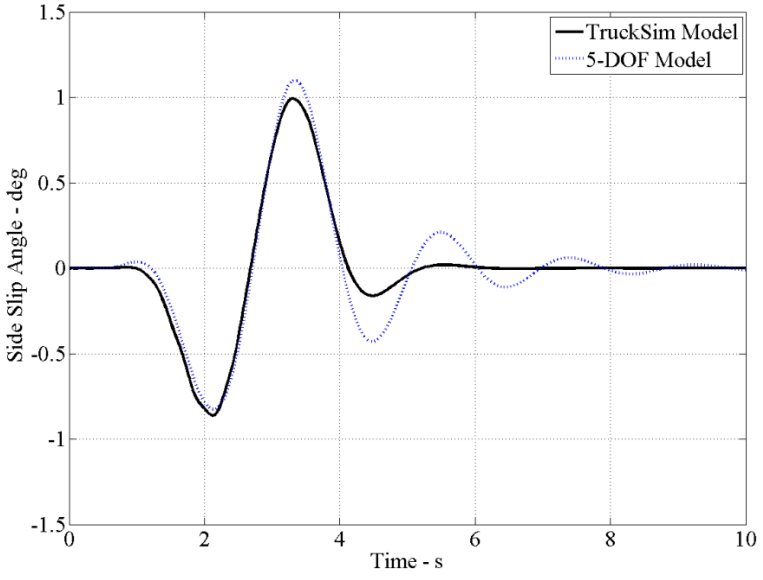

Figure 4.5: Semi-trailer side slip angle versus time

The lateral accelerations of the tractor and semi-trailer are shown in figure 4.6 and 4.7, respectively. The time histories for the two models agree very well. In the case of TruckSim models the maximum peak values of lateral accelerations of the tractor and semi-trailer were approximately 0.15g and 0.17g, respectively. The yaw rates for the tractor and semi-trailer for the two models are shown in figure 4.8 and 4.9. Again the yaw rate time histories of the two models agree very well. In the case of TruckSim models, the maximum peak values of yaw rate of the tractor and semi-trailer were approximately 4.5 deg/s and 5.5 deg/s, respectively.

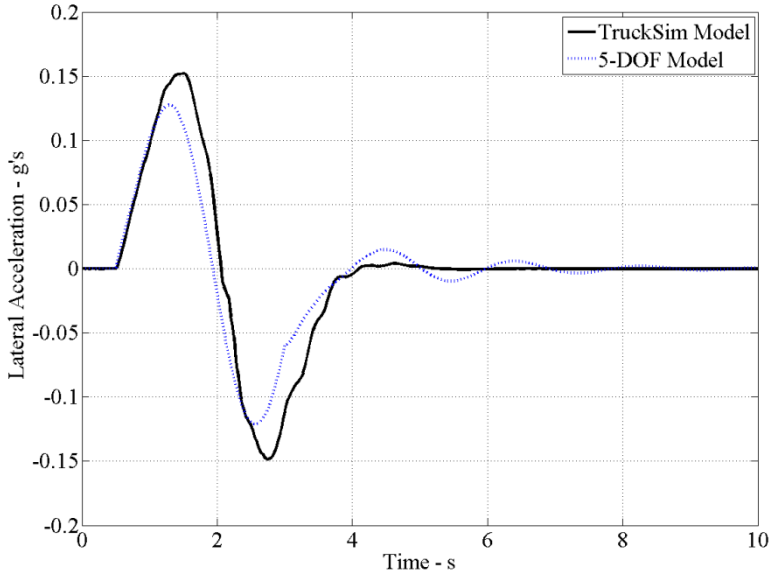

Figure 4.6: Tractor lateral acceleration versus time

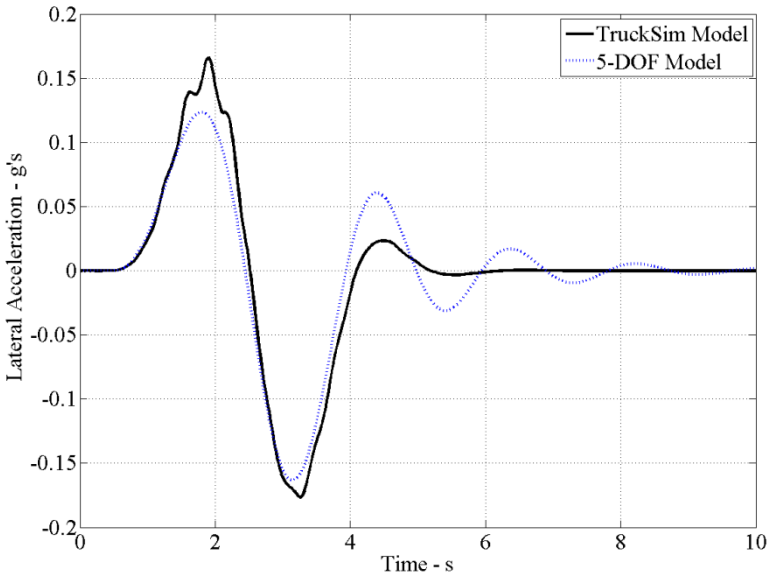

Figure 4.7: Semi-trailer lateral acceleration versus time

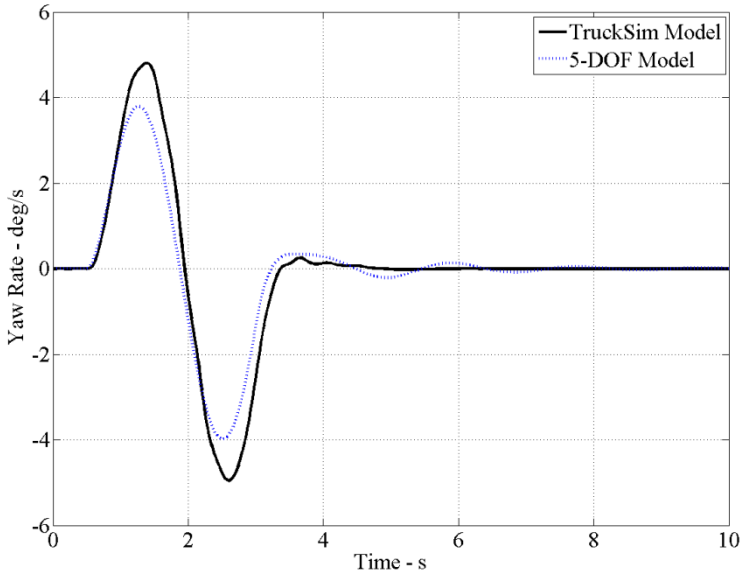

Figure 4.8: Tractor yaw rate versus time

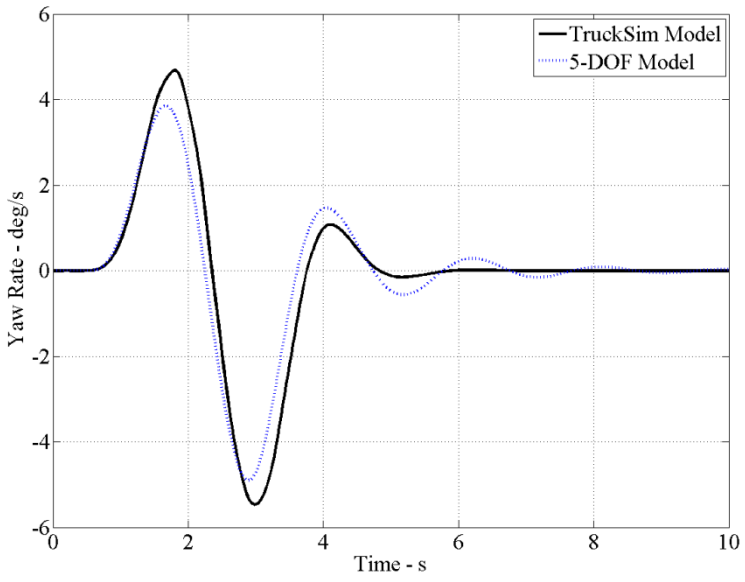

Figure 4.9: Semi-trailer yaw rate versus time

In figures 4.4 – 4.9, a steady oscillation is observed at the end of the dynamic manoeuvre for the tractor and semi-trailer of the 5-DOF linear model. This can be explained by the fact that no steering compliance was included in the 5-DOF linear model.

4.4.2 ARSC SYSTEM PERFORMANCE

Based on the validated 5-DOF vehicle model, an active roll stability control (ARSC) system is developed for AHVs. The roll stability of the AHV with the ARSC system was investigated. The testing manoeuvre emulated is the open-loop single lane change at the speed of 88 km/hr as described in section 3.5.1.

Figure 4.10 shows the simulated roll angle response of the tractor for both the passive system and the active controlled system. The peak values of roll angle of the

passive system and the active controlled system are 3.4658^0 and 0.5589^0, respectively. Figure 4.11 shows the simulated roll angle response of the semi-trailer for both the passive system and the active controlled system. The peak values of roll angle of the passive system and the active controlled system are 5.3302^0 and 0.8389^0, respectively. It is also observed that in figures 4.10 and 4.11, the active controlled system dampened out oscillations at the end of the testing manoeuvre, while oscillations were present in the passive system.

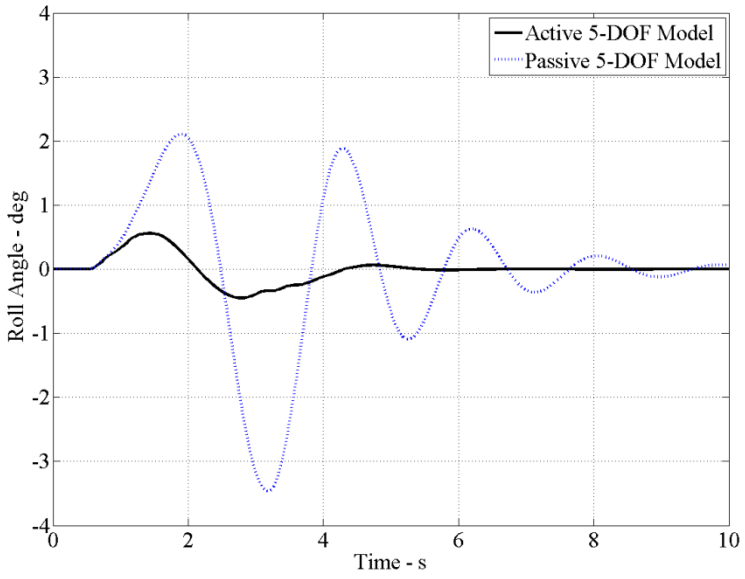

Figure 4.10: Tractor roll angle versus time

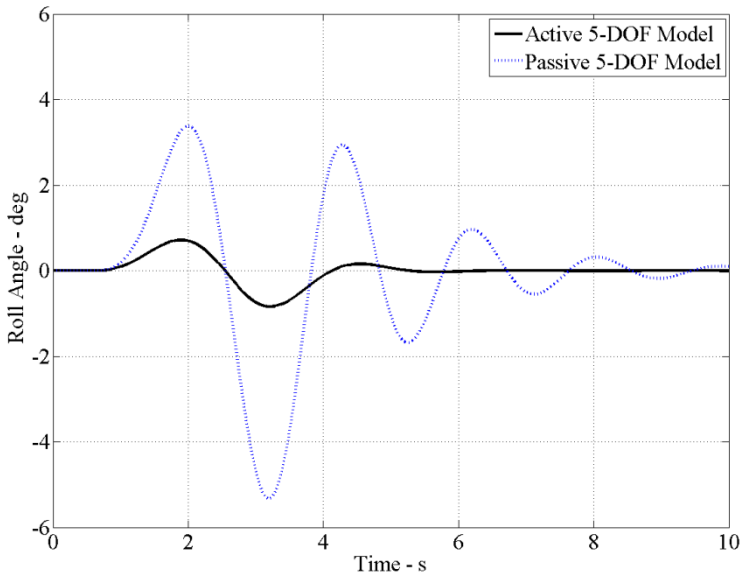

Figure 4.11: Semi-trailer roll angle versus time

Figure 4.12 shows the simulated axle roll angle response of the tractor for both the passive system and active control system. The peak values of axle roll angle of the passive system and the active controlled system are 0.3855^0 and 0.1500^0, respectively.

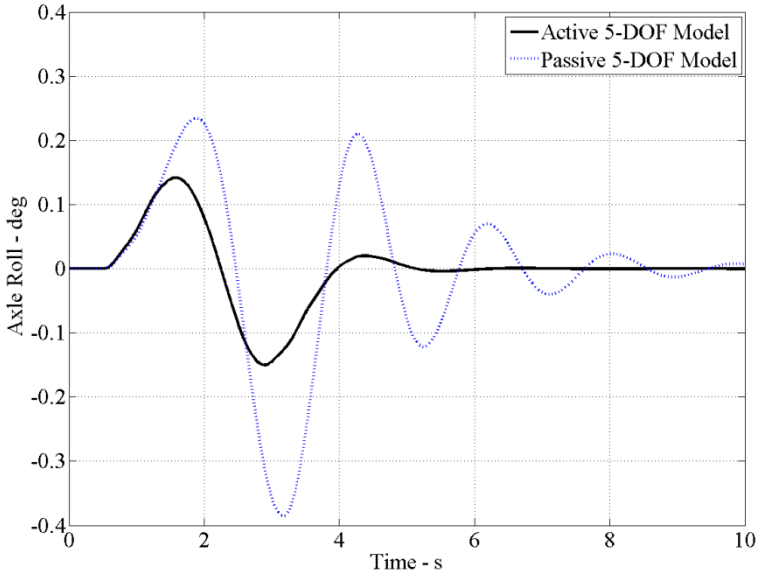

Figure 4.12: Tractor axle roll angle versus time

Figure 4.13 shows the simulated axle roll angle response of the semi-trailer for both the passive system and the active control system. The peak values of axle roll angle of the passive system and the active controlled system are 0.6584^0 and 0.3177^0, respectively.

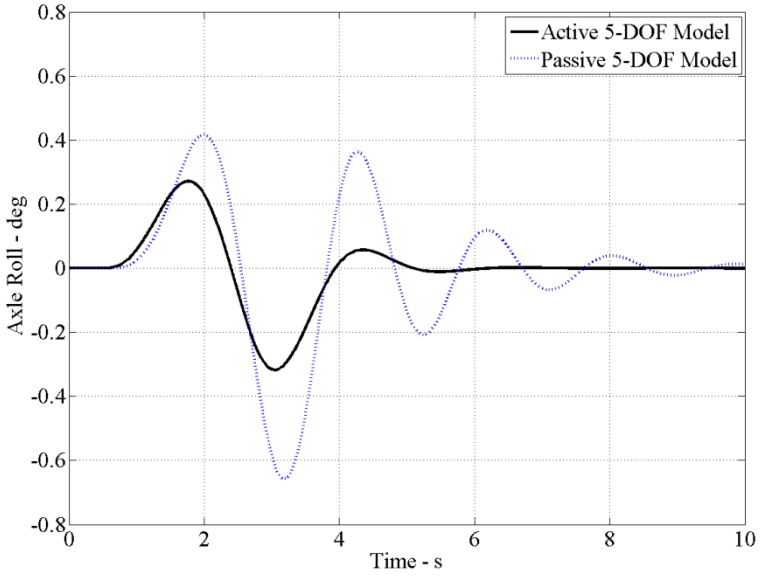

Figure 4.13: Semi-trailer axle roll angle versus time

It is again observed that in figures 4.12 and 4.13, the active controlled system dampened out oscillations at the end of the dynamic manoeuvre, while oscillations were present in the passive system.

Figures 4.14 and 4.15 compare the tractor and semi-trailer yaw rate for the passive system and the active system, respectively. It is observed that the two yaw rate time histories are almost the same under the dynamic manoeuvre, but the active control system has dampened out oscillations at the end of the manoeuvre, while oscillations were present in the passive system.

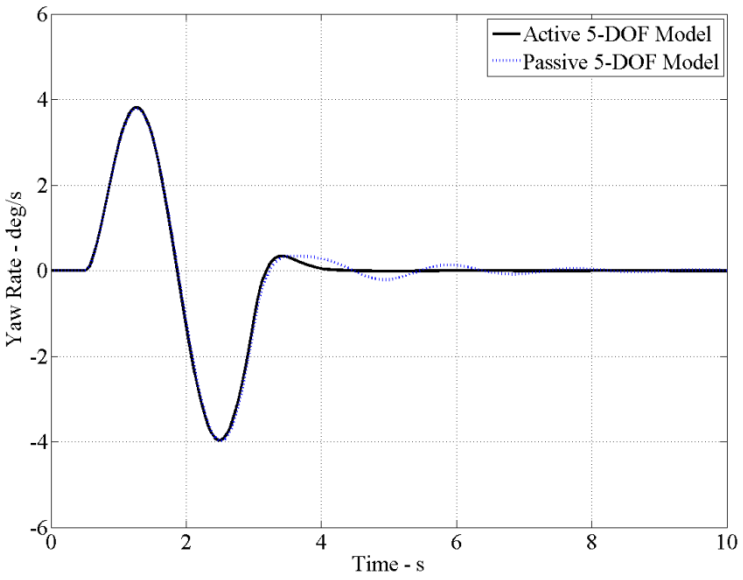

Figure 4.14: Tractor yaw rate versus time

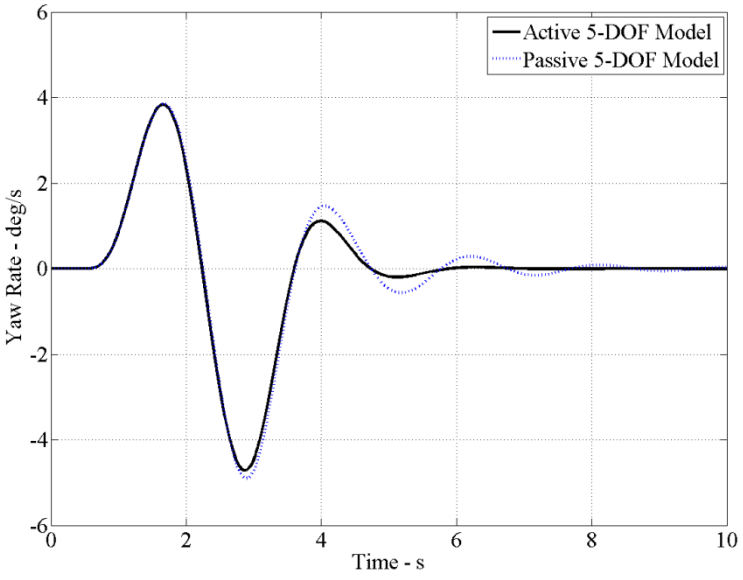

Figure 4.15: Semi-trailer yaw rate versus time

The side slip angle for the tractor and semi-trailer are compared for the passive system and the active system in figures 4.16 and 4.17, respectively. It is observed that the two side slip time histories are almost the same under the testing manoeuvre, but the active controlled system has lower peaks and almost damped oscillations at the end of the manoeuvre, while oscillations were present in the passive system.

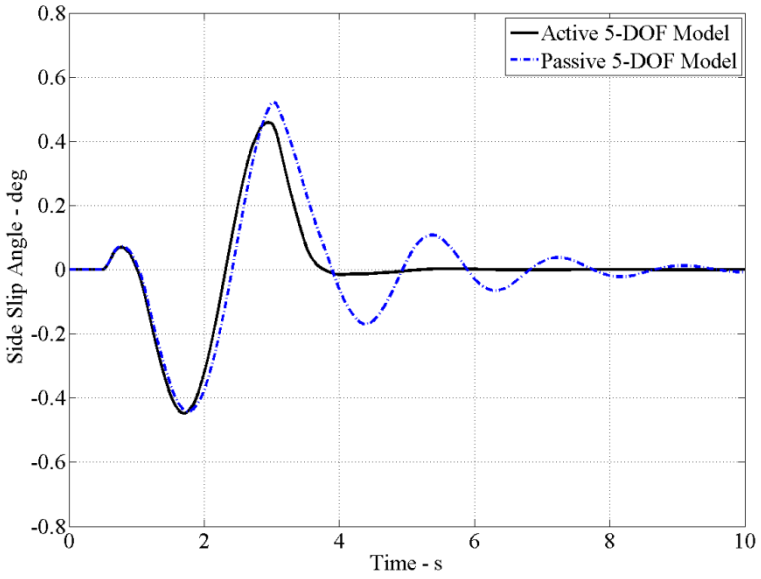

Figure 4.16: Tractor Side slip angle versus time

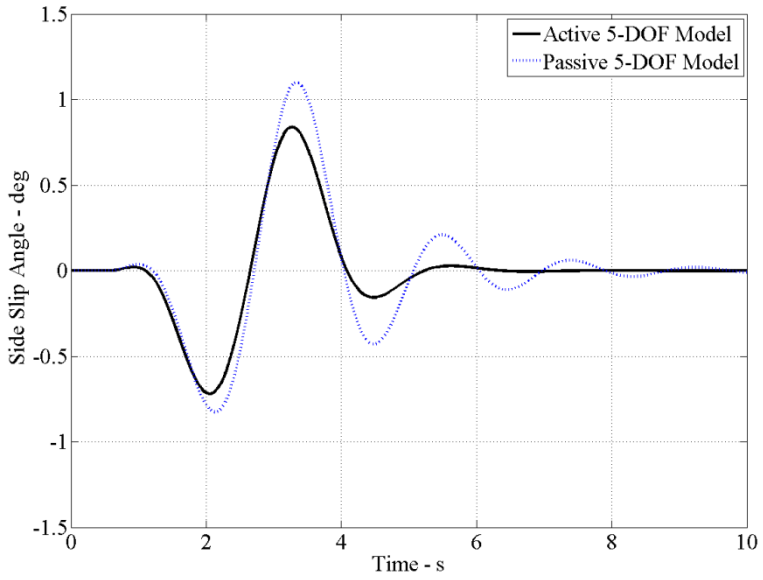

Figure 4.17: Semi-trailer side slip angle versus time

Figures 4.18 and 4.19 show the lateral acceleration time histories of the tractor and semi-trailer for both the passive system and the active controlled system, respectively. It is observed that the passive system vehicle units would roll outwards during the dynamic manoeuvre. But the active control system counters this outward roll and tends to make the vehicle units roll inwards during the dynamic manoeuvre. It is also noted that the active controlled system almost eliminates unwanted oscillations at the end of the manoeuvre.

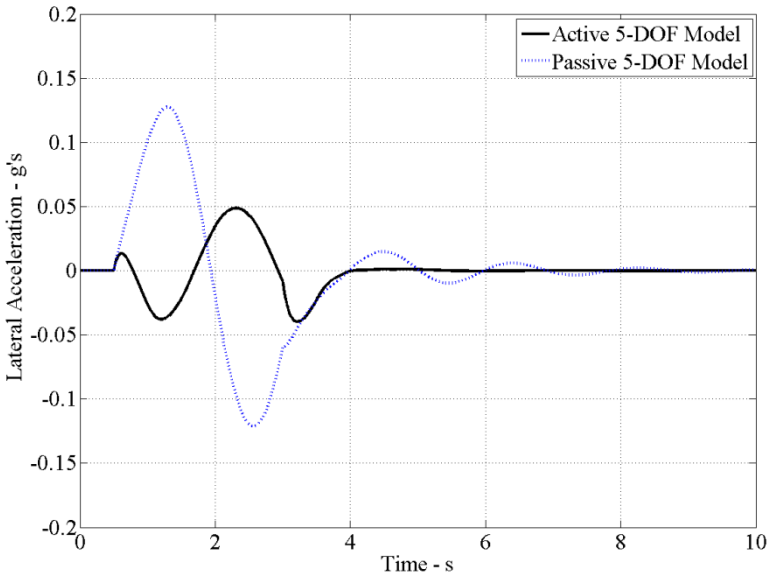

Figure 4.18: Tractor lateral acceleration versus time

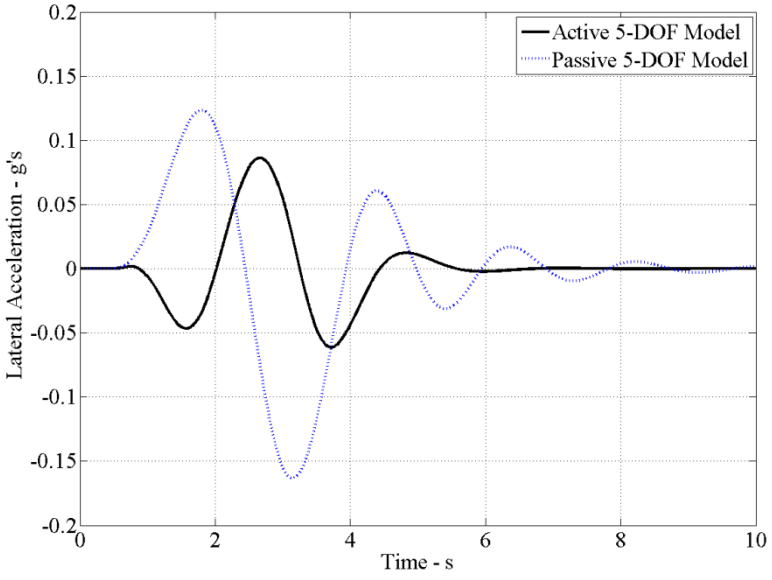

Figure 4.19: Semi-trailer lateral acceleration versus time

The roll rate for the tractor and semi-trailer are compared for the passive system and the active system in figures 4.20 and 4.21, respectively. It is observed from the two roll angle time histories that the active controlled system has dampened out the roll rate of the two vehicle units during the manoeuvre. The active control system has also eliminated oscillations at the end of the dynamic manoeuvre, while oscillations were present in the passive system.

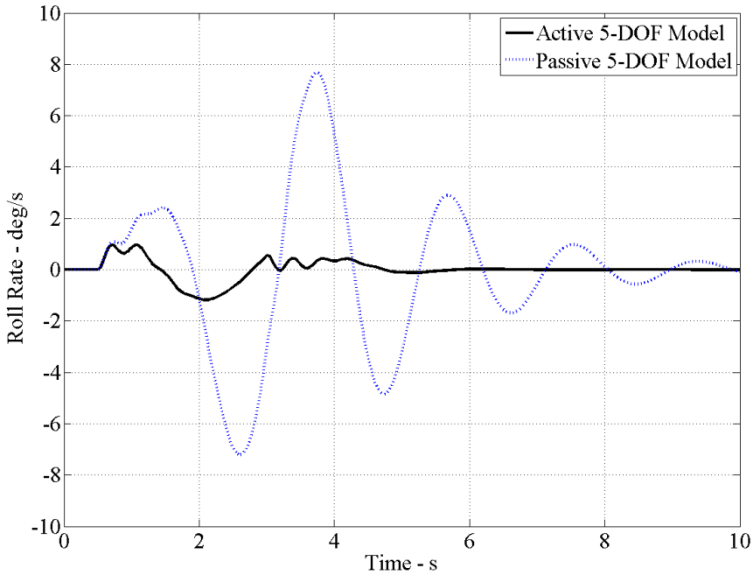

Figure 4.20: Tractor roll rate versus time

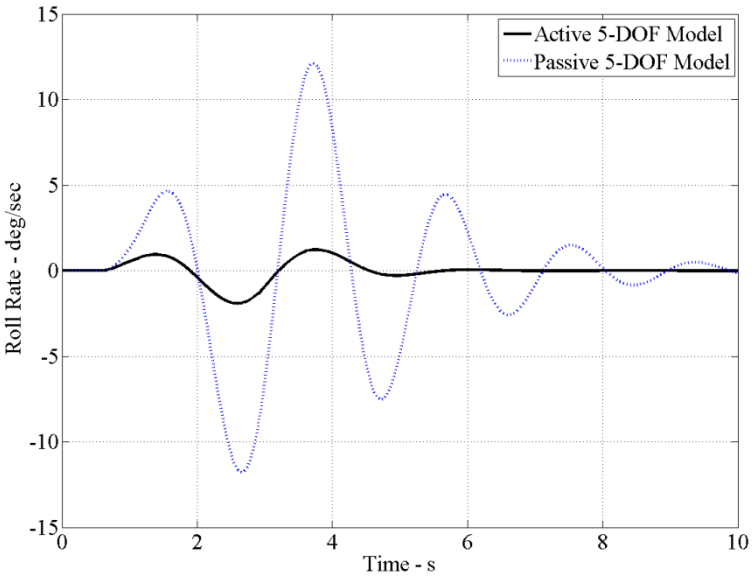

Figure 4.21: Semi-trailer roll rate versus time

The time histories of control input and energy consumption are given in figures 4.22 and 4.23, respectively.

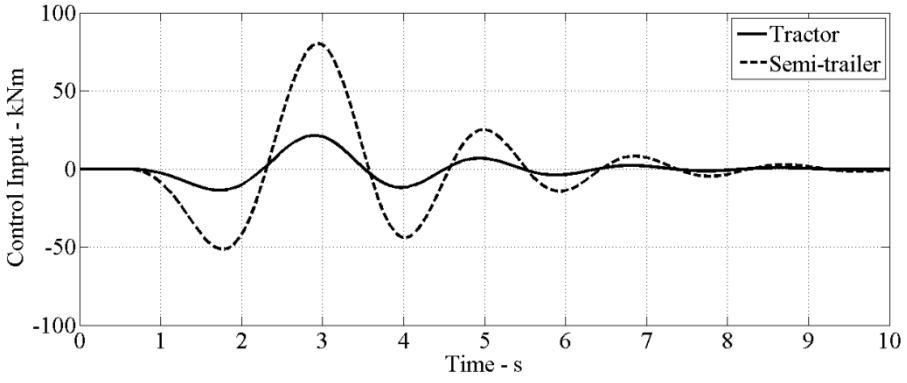

Figure 4.22: Control input time history

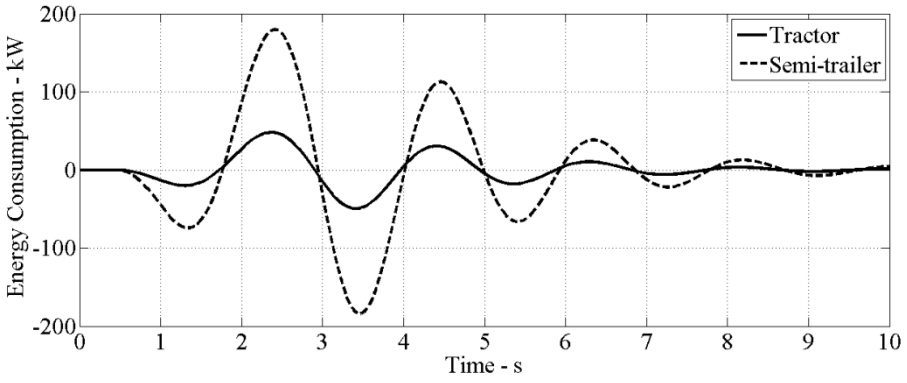

Figure 4.23: Energy consumption time history

Table 4.2 summarizes the improvements in roll stability of the AHV using the anti roll stability control system.

Table 4.2: Summary of the improvements in roll stability of AHV using the ARSC system

	Tractor Roll Angle	Semi-trailer Roll Angle	Tractor Axle Roll Angle	Semi-trailer Axle Roll Angle
Passive Vehicle	3.4658^0	5.3302^0	0.3855^0	0.6584^0
Active Controlled Vehicle	0.5589^0	0.8389^0	0.1500^0	0.3177^0
% Improvement	83.87%	84.26%	61.1%	51.75%

4.5 SUMMARY

A 3D yaw/roll AHV model is presented. This is a linear model with five degrees of freedom, considering lateral, yaw and roll motions of the tractor and the yaw and roll motions of the semi-trailer. An active anti-roll bar suspension system is developed and incorporated into the active roll stability control (ARSC) system. A controller for the ARSC system is designed using the linear quadratic regulator technique. The designed LQR controller has improved the tractor roll by 83.87% and the semi-trailer roll by 84.26%. With the ARSC system, the tractor axle roll and the semi-trailer axle roll are also improved by 61.1% and 51.75%, respectively.

CHAPTER 5

DESIGN OPTIMIZATION OF AHVs FOR IMPROVING DIRECTIONAL PERFORMANCE

5.1 INTRODUCTION

This chapter presents a design optimization method for AHVs using genetic algorithms (GAs) and multibody vehicle system models. Among all conflicting design goals of AHVs, the trade-off relationship between manoeuvrability at low speeds and lateral stability at high speeds is the most fundamental and important, which bothers vehicle designers and researchers. Path following off-tracking (PFOT) and rearward amplification (RWA) ratio are the important performance measures for the manoeuvrability and stability, respectively. A design optimization method based on a GA and a multibody vehicle dynamic package, TruckSim, is proposed to coordinate this trade-off relationship.

5.2 TRUCKSIM SOFTWARE PACKAGE

TruckSim is a commercialized simulation program based on the Windows operating system platform. It can be licensed from the Mechanical Simulation Corporation, Ann Arbor. TruckSim can be used to simulate and analyze the dynamic behaviors of buses, trucks and articulated vehicles in response to user defined accelerations, steering, braking and road profile inputs.

TruckSim software consists of four distinct modules namely,

- VehicleSim browser (VS browser)
- VehicleSim solver (VS solver)
- Surface animator (SurfAnim)
- Engineering plotter for Windows (WinEP)

The VS browser is a graphical user interface (GUI) which works as the primary interface to TruckSim. It consists of a collection of databases. These databases are used to define vehicle model parameters, control inputs and simulation settings. The VS solver is a collection Windows Dynamic Link Library (DLL) files. It is used to solve the relevant equations of the vehicle model and execute the user defined dynamic simulation. SurfAnim is used to visually see and analyze the simulated run. The user can interactively zoom in and out with a simulated camera and also move around the simulated vehicle to change the point of view. WinEP is used to create plots of vehicle variables as defined by the user. Any variable computed by the simulation model can be plotted using WinEP. The four above mentioned modules are schematically shown in figure 5.1. Further details for TruckSim program can be found in the TruckSim reference manual [100].

Figure 5.1: Schematic diagram of TruckSim software functionality

Each time a simulation is carried out, TruckSim saves all the simulation data in the ERD (Engineering Research Division) file format. ERD of the University of Michigan Transport Research Institute (UMTRI) developed this file format to support automated plotting of simulation and test data.

An ERD file consists of two independent sections, the header and the data. The header section contains only text and is an ordinary text file with the extension ERD.

On the other hand, the data section contains only numbers in the binary format and is a binary file with the extension BIN.

5.2 INTERFACING TRUCKSIM AND MATLAB

TruckSim's VS browser can be used as an *ActiveX* server which allows other Windows based applications access via a component object model (COM) interface. This COM interface of the VS browser serves as its *application program interface* (API).

The first step is to register the *automation server*. To register TruckSim, the following command is used in the Windows command window:

{TruckSim prog folder}\TruckSim.exe /RegServer

Once this is done, TruckSim can now be started from the COM client software (Matlab) using the following command:

h = actxserver('TruckSim.Application')

By registering the automation server, the API can be used to bypass the VS browser GUI and run the VS solver under the control of Matlab.

To perform GA optimization using a selected TruckSim vehicle model and Matlab's optimization toolbox, the instructions described above are followed along with the following tweaks in TruckSim, as shown in figure 5.2.

- The VS solver is transferred to the Windows local directory.

- A configuration file is defined and saved using the ERD File Converter. This configuration file depends on the vehicle model selected in TruckSim and is defined such that the output variables (data) required by Matlab are converted from the ERD file format to Matlab's MAT file format.

- In TruckSim, the writing channels are enabled and the same output variables are again defined as was defined in the configuration file in the above step.

- The final step is to define the path of the configuration file in TruckSim.

Now the two software packages are integrated and ready to perform GA optimization.

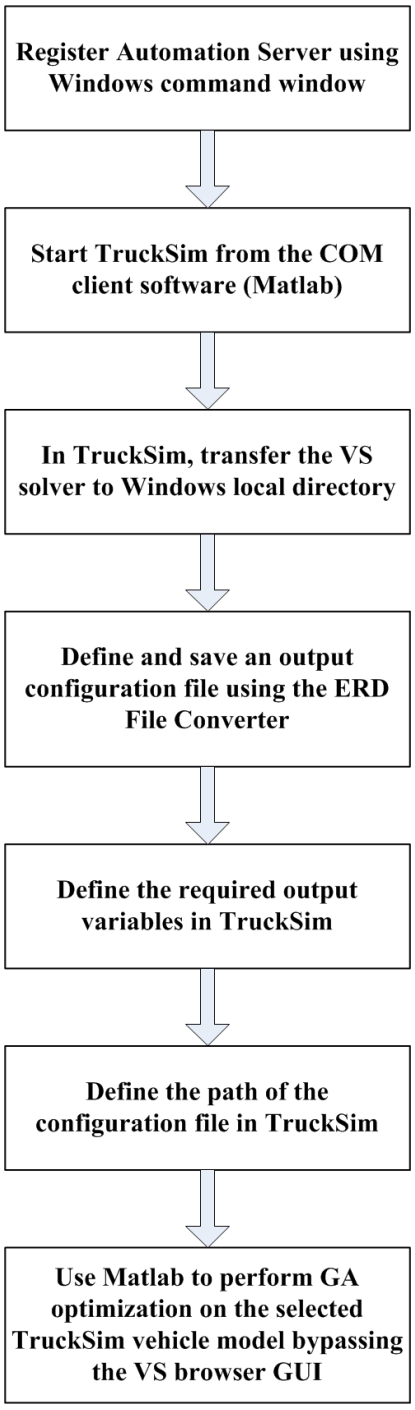

Figure 5.2: Steps to interface TruckSim and Matlab to perform GA optimization

5.3 TRUCKSIM VEHICLE MODEL

An AHV with a tractor and one semi-trailer combination as shown in figure 5.3 is selected. The corresponding multibody vehicle model from TruckSim is used to conduct numerical simulations. The vehicle modeling is based on UMTRI's constant velocity yaw/roll program [96].

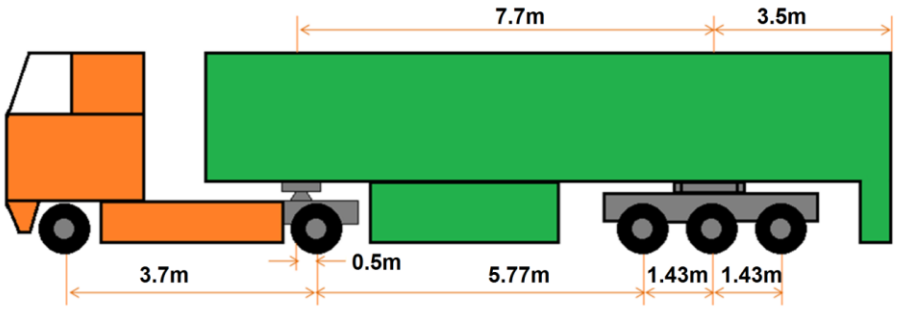

Figure 5.3: Schematic diagram of the selected TruckSim AHV model

The total number of degree of freedom of the selected articulated vehicle is eighteen. The tractor sprung mass is treated as a rigid body with five degrees of freedom, namely, lateral, vertical, pitch, roll and yaw. The semi-trailer sprung mass is also treated as a rigid body with three degrees of freedom, namely, pitch, roll and yaw. Each axle has two degrees of freedom. The forward velocity of the tractor is assumed to remain constant during any manoeuvre and so the longitudinal degree of freedom is not included. Each axle is treated as a beam axle which can roll and bounce with respect to the sprung mass to which it is attached. All other suspension motions, such as pitch, camber, lateral position, etc., are nonlinear properties represented as tabular function. Also the nonlinear cornering force and aligning torque characteristics of the tire are represented as tabular functions.

5.4 SIMULATION AND RESULTS

The selected AHV with a tractor and a semi-trailer is optimized based on the design criteria: the PFOT is minimized while maintaining the RWA ratio as close as possible to 1.0.

There are ten design variables, namely, sprung mass of tractor m_{s1}, sprung mass of semi-trailer m_{s2}, tractor wheelbase l_1, semi-trailer wheelbase l_2, unsprung mass of axle 1 m_{u1}, unsprung mass of axle 2 m_{u2}, unsprung mass of axle 3 m_{u3}, track of axle 1 t_1, track of axle 2 t_2 and track of axle 3 t_3. The three tridem axles of the semi-trailer are considered as a single axle, namely, axle3. The nominal geometric parameter values are selected as shown in Figure 5.3. Other parameters' nominal values are provided in Appendix B.

The design optimization problem is formulated to search a set of optimal values of the above ten design variables in order to minimize the following objective function value [97, 98]:

$$\text{Obj} = \delta_1 \times \left| \text{RWA} - 1 \right| + \delta_2 \times \text{PFOT} \tag{5.1}$$

where, δ_1 and δ_2 are the weight factors and both of them take the value of 1.0. To evaluate the fitness value of the objective function shown in equation (5.1), the performance measure of PFOT is determined under the low speed corner swept path width (SPW_{90}) manoeuvre. The RWA ratio is obtained in the single lane change manoeuvre specified by SAE J2179.

The design optimization is implemented as illustrated in figure 5.4.

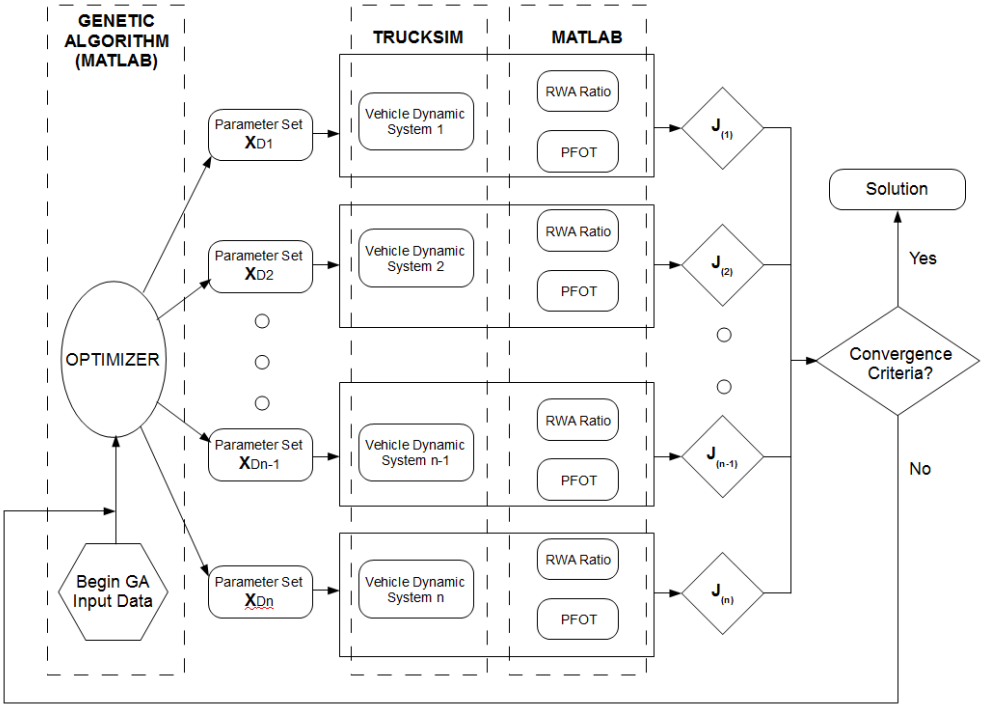

Figure 5.4: Block diagram of the design optimization implementation

First, a population of n sets of design variables is randomly selected by the GA in Matlab and given to the GA optimizer; the optimizer sends this data to the multibody vehicle dynamics software TruckSim where the multibody vehicle model is updated. Then, the vehicle model simulates to travel in both the high-speed single lane change manoeuvre and the low-speed corner swept path width (SPW_{90}) manoeuvre, respectively. Each manoeuvre is a closed loop simulation within TruckSim involving the built-in driver model which imitates the driving response of a human driver as shown in figure 5.5.

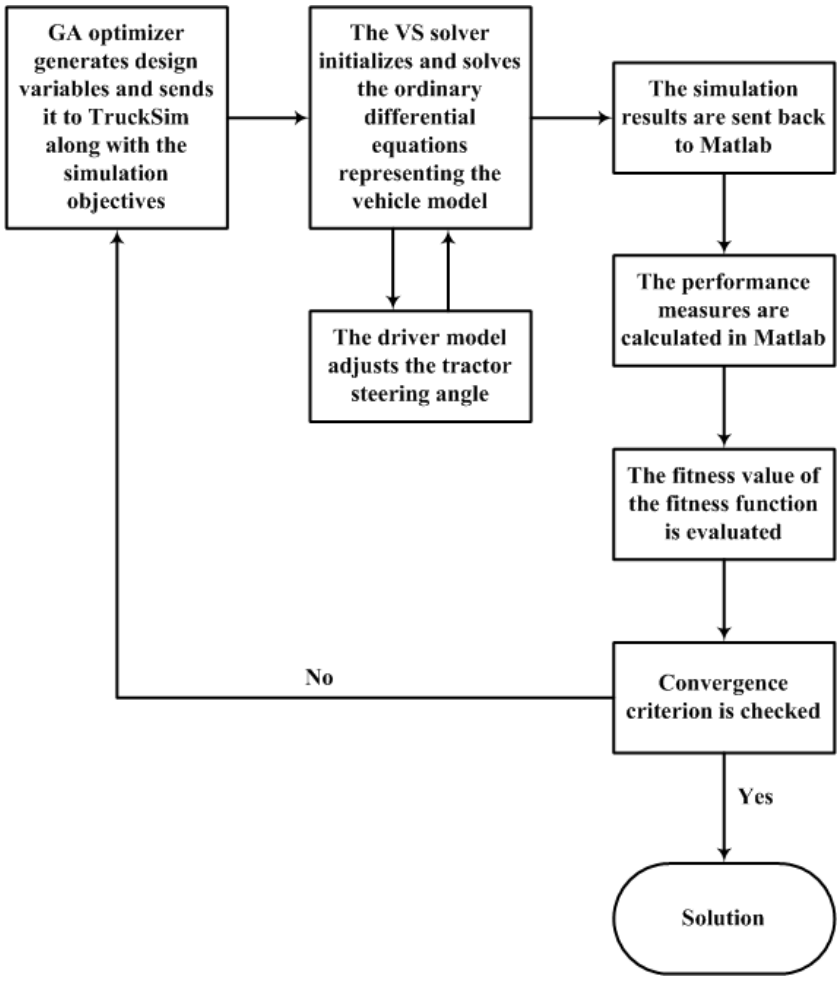

Figure 5.5: Closed loop simulation process in TruckSim

Simulation data is sent back to Matlab according to the procedure described in section 5.2, where the corresponding data processor determines the resulting performance measure, RWA ratio and PFOT value. These performance measures are used to construct the objective function shown in equation (5.1) to evaluate the required fitness value. At this point, if the convergence criteria are satisfied, the calculation stops; otherwise, the resulting fitness value is sent back to the GA. Based on the returned fitness value corresponding to the given set of design variables, the GA produces the next generation of design variable sets using selection, crossover,

and mutation operators. This procedure repeats until the optimized variable set is found.

In the design optimization, the GA parameters of crossover rate, population number and total generation number take the values of 0.8, 40 and 60 respectively. Gaussian function is selected for the mutation operator. The design variable upper and lower bounds are set as +10% and -10% varied from the nominal value for each of the ten design variables, respectively. The optimized design variables and performance measures are listed in Table 5.1. For the purpose of comparison, the nominal values of the design variables and the corresponding performance measures are also listed in the table.

Table 5.1: Comparison chart of the different simulations

	Simulation using nominal values	Simulation using values obtained with GA	
m_{s1} (kg)	6179	5791	
m_{s2} (kg)	29090	26219	
l_1 (mm)	3700	3565	
l_2 (mm)	7700	7286	
m_{u1} (kg)	527	479	
m_{u2} (kg)	1004	920	
m_{u3} (kg)	2205	2337	
t_1 (m)	2022	1922	
t_2 (m)	1829	1965	
t_3 (m)	2140	2264	% Improvement
RWA	1.22	1.14	6.56%
PFOT (mm)	2733	2506	8.31%

Figures 5.6 and 5.7 illustrate the lateral accelerations at the CGs of the tractor and semi-trailer in the baseline case and the optimized case respectively. In the baseline case, the RWA ratio takes the value of 1.22, whereas in the optimized case, the ratio is equal to 1.14, an improvement of 6.56%.

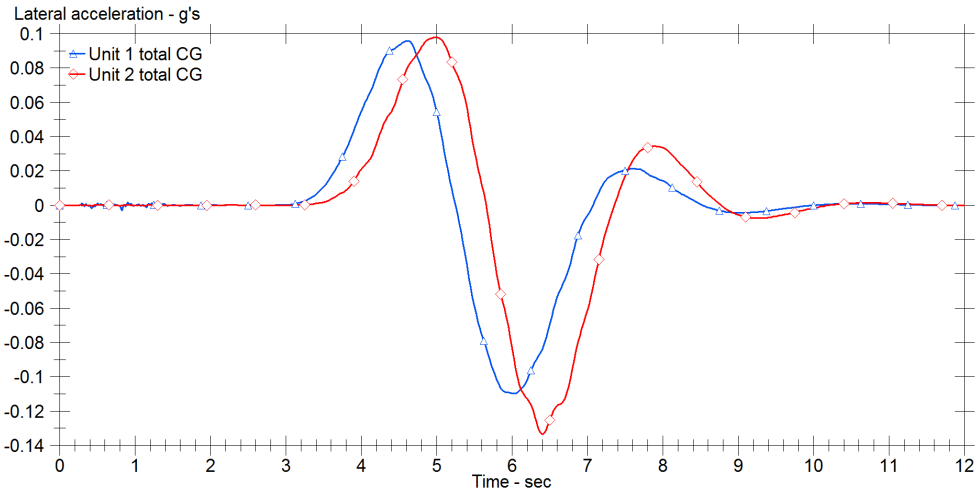

Figure 5.6: Lateral accelerations at CGs of tractor and semi-trailer versus time for the baseline design

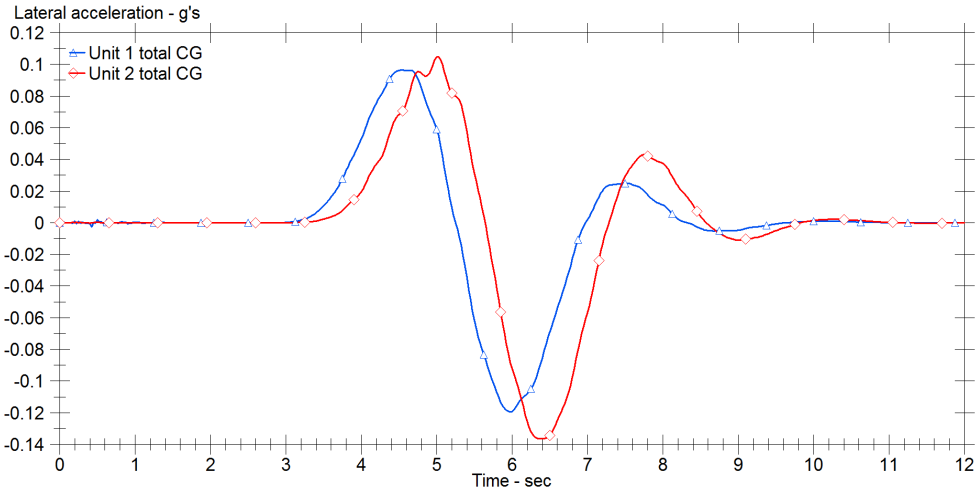

Figure 5.7: Lateral accelerations at CGs of tractor and semi-trailer versus time for the optimized design

Figures 5.8 and 5.9 illustrate the trajectories of the tractor and semi-trailer in the baseline case and the optimized case respectively. In the optimized design case, the PFOT value is 2506 mm, while in the baseline design the value of PFOT is 2733 mm, an improvement of 8.31%.

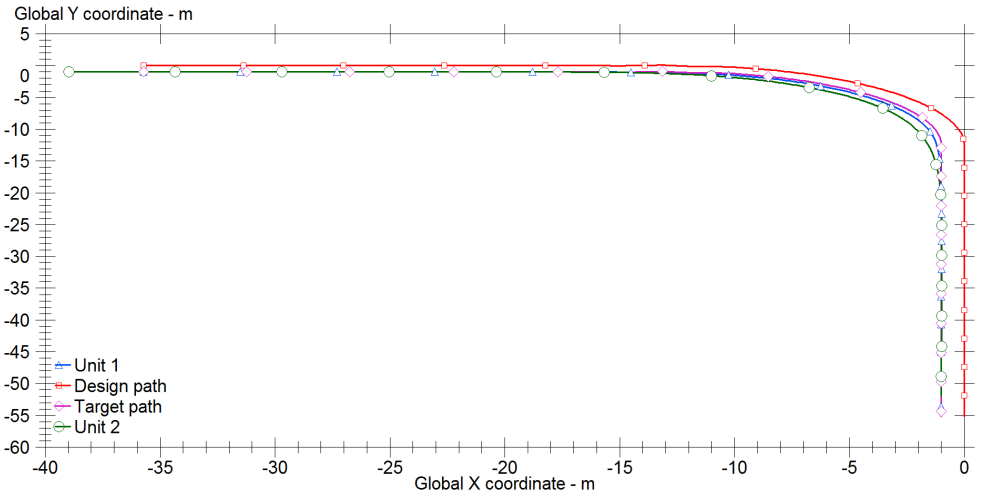

Figure 5.8: Trajectories of tractor and semi-trailer for the baseline design

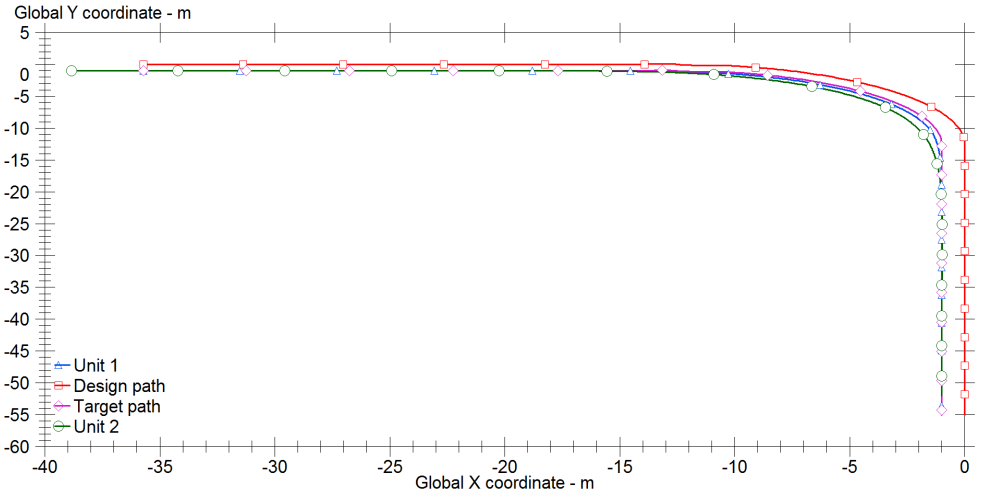

Figure 5.9: Trajectories of tractor and semi-trailer for the optimized design

Figures 5.10 and 5.11 show the tractor side slip angle of optimized and baseline cases for both high-speed single lane change manoeuvre and low-speed SPW90^0 turn manoeuvre, respectively.

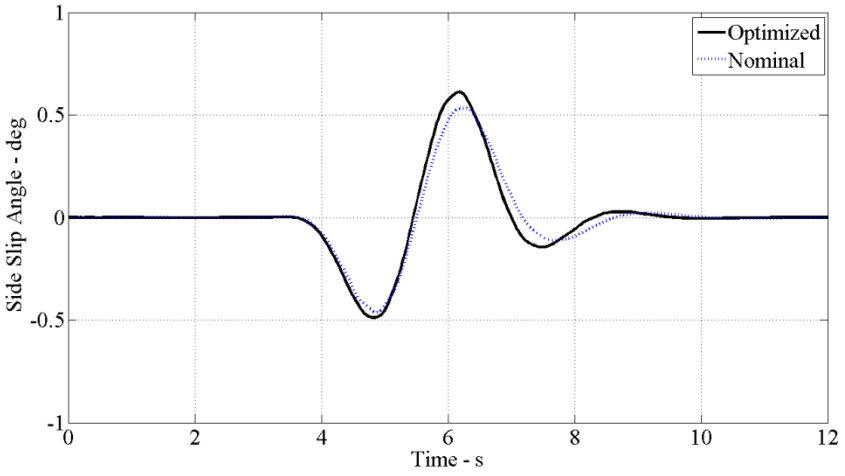

Figure 5.10: Tractor side slip angle versus time (high-speed manoeuvre)

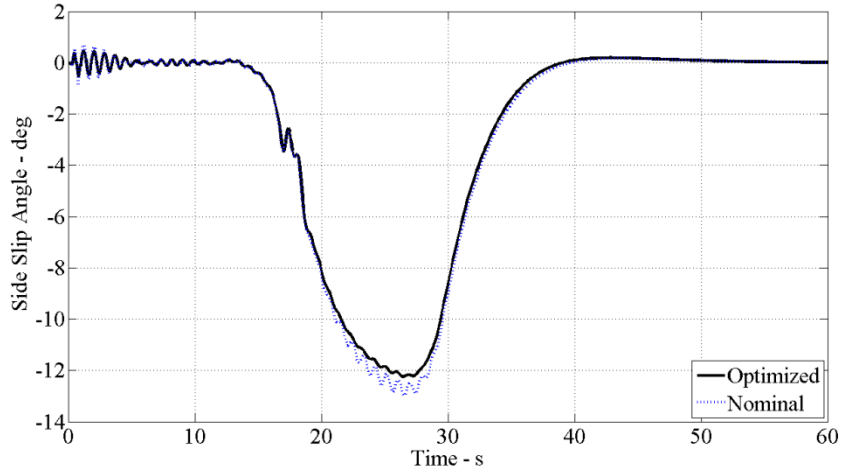

Figure 5.11: Tractor side slip angle versus time (low-speed manoeuvre)

Figures 5.12 and 5.13 show the semi-trailer side slip angle of optimized and baseline cases for both high-speed single lane change manoeuvre and low-speed SPW90^0 turn manoeuvre, respectively. From the time histories of figures 5.10 – 5.13, it is observed that the GA has selected the optimal design variables and

simultaneously reduces high-speed RWA ratio and low-speed PFOT without adversely changing the lateral dynamics of the AHV.

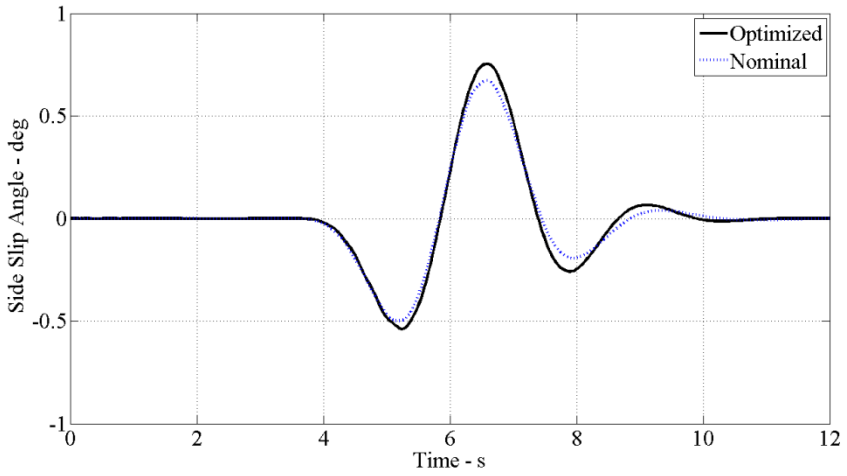

Figure 5.12: Semi-trailer side slip angle versus time (high-speed manoeuvre)

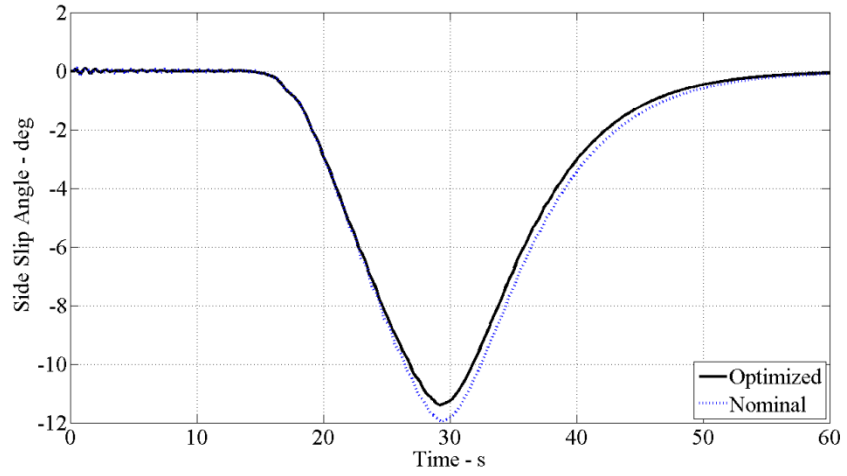

Figure 5.13: Semi-trailer side slip angle versus time (low-speed manoeuvre)

Figures 5.14 and 5.15 show the tractor yaw rate of optimized and baseline cases for both high-speed single lane change manoeuvre and low-speed SPW90^0 turn manoeuvre, respectively.

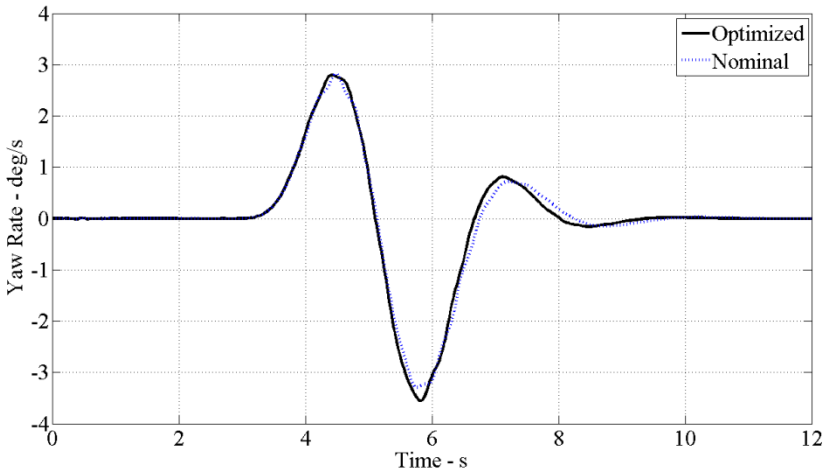

Figure 5.14: Tractor yaw rate versus time (high-speed manoeuvre)

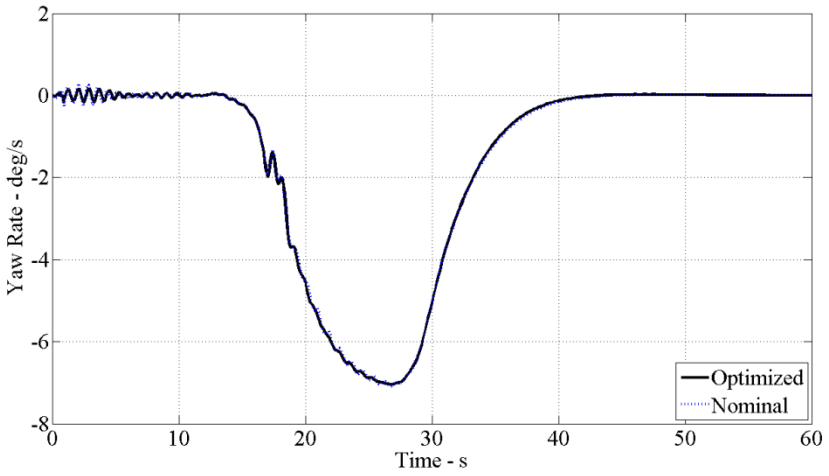

Figure 5.15: Tractor yaw rate versus time (low-speed manoeuvre)

Figures 5.16 and 5.17 show the semi-trailer yaw rate of optimized and baseline cases for both high-speed single lane change manoeuvre and low-speed SPW90^0 turn manoeuvre, respectively.

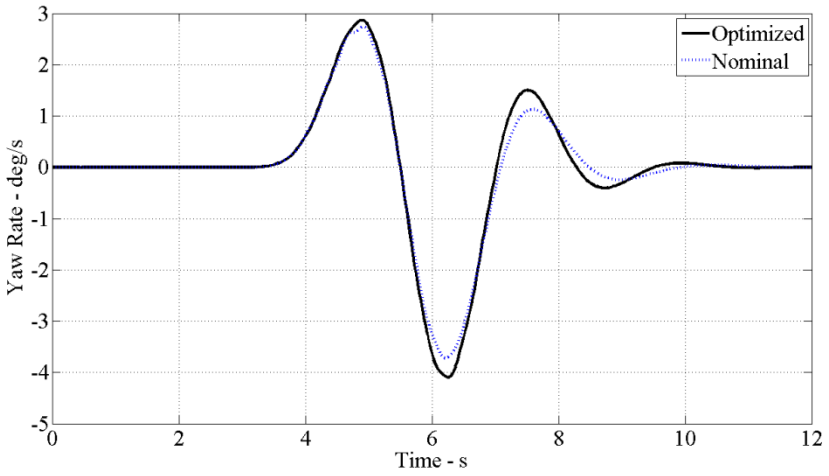

Figure 5.16: Semi-trailer yaw rate versus time (high-speed manoeuvre)

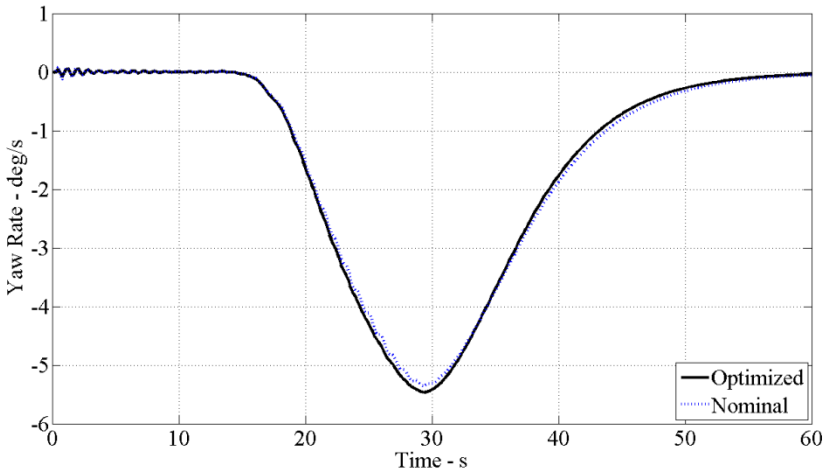

Figure 5.17: Semi-trailer yaw rate versus time (low speed manoeuvre)

From the time histories of figures 5.14 – 5.17 it is again observed that the GA has selected the optimal vehicle design variables and simultaneously reduces high-speed RWA ratio and low-speed PFOT without adversely changing the lateral dynamics of the AHV.

As shown in table 5.1, the optimized values of wheelbase of the tractor and semi-trailer are lower than the corresponding nominal values. This reduction in wheelbase contributes to the improvement of the vehicle manoeuvrability for the optimized case. This is aligned with the accepted conclusion that the shorter the vehicle wheelbase, the better the vehicle manoeuvrability. Whereas, the overall lower values of optimized mass variable and the increased axle2 and axle3 tracks help reduce RWA ratio for the high speed testing manoeuvre.

5.5 SUMMARY

This chapter presents a design optimization method for AHVs using GAs and multibody vehicle system models. To test the effectiveness of the design method an AHV a tractor with and semi-trailer combination is optimized using a proposed method. The objective of this vehicle design problem is to minimize low speed PFOT while keeping the high speed RWA ratio as close as possible to one. Based on the achieved results, GA has decreased the PFOT by 8.31% and the RWA ratio by 6.56%. It is indicated that the conflicting design criteria of low-speed manoeuvrability and high-speed stability can be simultaneously improved using the effective optimization

method. The proposed approach may be used for identifying desired design variables and predicting performance envelopes in the early design stages of AHVs.

CHAPTER 6

CONCLUSIONS

6.1 INTRODUCTION

As discussed in chapter 1 there are two objectives of this research. The first objective is to develop an active roll stability control (ARSC) system and the second one is to develop a novel method for the design synthesis of AHVs using realistic nonlinear vehicle models. This nonlinearity in the vehicle models is attributed to the nonlinear tire properties and the nonlinear suspension properties of the AHVs. Numerical analysis reveals that the two goals have been successfully achieved. The proposed ARSC system is believed to be a significant contribution to improve high-speed roll stability of AHVs. The proposed design synthesis method of AHVs is also considered to be an important contribution to design optimization of AHVs in the early stages of its design.

The achievements of the research and the scope of future research are addressed in this chapter.

6.2 ACTIVE ROLL STABILITY CONTROL

A 3-dimensional yaw/roll model is developed. This 5-DOF linear model is validated by comparing the simulation results based on this model with those using the linearized multibody vehicle model from TruckSim. The 5-DOF linear model is

validated for its dynamic performance while performing an open loop high speed single lane change manoeuvre. The two vehicle models are compared in terms of the lateral accelerations, the side slip angles, and the yaw rate. The discrepancies between the two models are attributed to no steering compliance in the 5-DOF linear model.

The validated linear model is used to design an active roll stability control (ARSC) system. The ARSC controller is designed based on the Linear Quadratic Regulator (LQR) Technique and is considered to be an active suspension consisting of hydraulic actuators in series with the anti-roll bar of the vehicle unit.

The designed LQR controller has improved the tractor roll by 83.87% and the semi-trailer roll by 84.26%. Also the tractor axle roll and the semi-trailer axle roll are improved by 61.1% and 51.75%, respectively, when compared with the baseline suspension. It is observed that with the proposed design, the rollover threshold of the vehicle can by greatly increased without drastically changing its handling performance.

6.3 DESIGN OPTIMIZATION OF AHVs FOR IMPROVING DIRECTIONAL PERFORMANCE

A design optimization method for AHVs is developed using GAs and multibody vehicle system models. The novel approach is proposed to interface Matlab with TruckSim. This proposed method is used to optimize the system parameter of a tractor/semi-trailer model in TruckSim. This optimization is based on a genetic algorithm and is carried out using the *Optimization Toolbox* in Matlab.

The objective of this optimization problem is to minimize the low speed PFOT while keeping high speed RWA ratio as close as possible to 1.0. Closed-loop testing manoeuvres are emulated, i.e. a driver model is included in the vehicle dynamic simulations. PFOT is achieved from the swept path width 90^0 (SPW_{90}) turn manoeuvre, while the RWA ratio was attained from the high-speed single lane change manoeuvre specified in the SAE J2179 testing procedure.

The optimization results show that the GA decreases the vehicle's low-speed PFOT by 8.31% and reduces the high-speed RWA ratio by 6.56%. It is indicated that the conflicting design criteria of low-speed manoeuvrability and high-speed stability can be simultaneously improved using the effective optimization method. The proposed approach may be used for identifying desired design variables and predicting performance envelopes in the early design stages of AHVs.

6.4 RECOMMENDATIONS FOR FUTURE WORK

In the current research AHV models based on a tractor/semi-trailer combination are used for simulations. These vehicle models should be extended to include long combination vehicles (LCVs), consisting of a tractor and two trailers. Further recommendations are given in the sub-sections below.

6.4.1 ACTIVE ROLL STABILITY CONTROL

i. The sprung masses of the vehicle are assumed to be flexible. The influence of the torsional frame flexibility of the vehicle units equipped with active

suspension systems should be investigated for its handling dynamics and rollover performance.

ii. Closed-loop testing manoeuvres are simulated. A driver model should be developed and included in vehicle modeling. The LQR controller should be optimized for any practical vehicle speed and manoeuvre.

iii. Integrated control strategies based on a combination of active suspension, active steering and active differential braking should be investigated. It is believed that such system will achieve the best handling dynamics and rollover performance for AHVs.

6.4.2 DESIGN OPTIMIZATION OF AHVs

i. Sensitivity analysis should be conducted for the geometric parameters of the vehicle. This should give an understanding as to which parameters most influence the vehicle's low-speed and high-speed dynamic performance. With this understanding, the GA can be further tuned to obtain optimized vehicle parameters which exhibit the best dynamic performance for any vehicle manoeuvre.

ii. The proposed method is limited by the associated heavy computational burden. To overcome this, the use of parallel computing should be investigated and implemented. This can reduce the computation time by approximately a factor of the population size of the GA [99].

iii. Active control systems should be incorporated into the TruckSim vehicle model. The proposed optimization method can be readily used on such

modified active system models. It is believed that this will further help improve the vehicle's directional performance.

REFERENCES

[1] P. Fancher and C. Winkler. Directional performance issues in evaluation and design of heavy articulated vehicles. *Veh. Syst. Dyn. 45(7-8),* pp. 607–647. 2007.

[2] Anonymous Focus on freight. Department for Transportation. London, UK. 2006.

[3] H. Prem, Austroads and National Road Transport Commission (Australia). *Comparison of Modelling Systems for Performance-Based Assessments of Heavy Vehicles:(Performance Based Standards NRTC/Austroads Project A3 and A4)* 2001.

[4] C. B. Winkler. Heavy vehicle size and weight: Test procedures for minimum safety performance standards. Final technical report. UMTRI, Ann Arbor, Michigan, USA, 1992.

[5] M. El-Gindy, N. Mrad and X. Tong. Sensitivity of rearward amplification control of a tractor/full trailer to tyre cornering stiffness variable. *Proc.IMechE, Part D: J.Automobile Engineering 215*pp. 579-588. 2001.

[6] Anonymous "Rules for the assessment of potential performance-based standards. discussion paper," National Transport Commission (NTC), Australia, June 2005.

[7] Y. He, A. Khajepour, J. McPhee and X. Wang. Dynamic modelling and stability analysis of articulated frame steer vehicles. *International Journal of Heavy Vehicle Systems 12(1),* pp. 28-59. 2005.

[8] Anonymous Commercial driver handbook. California Department of Motor Vehicles. 2010-2011.

[9] S. McFarlane and P. Sweatman. The development of high productivity combination vehicles using computer simulation. *SAE Transactions 106*pp. 656-664. 1997.

[10] S. Rakheja, S. Sankar and R. Ranganathan. Roll plane analysis of articulated tank vehicles during steady turning. *Veh. Syst. Dyn. 17(1),* pp. 81-104. 1988.

[11] S. Rakheja, S. Sankar and R. Ranganathan. Influence of tank design factors on the rollover threshold of partially filled tank vehicles. *SAE Technical Paper 892480*1989.

[12] Anonymous "Road accidents in great-britain," Department of Transportation, HMSO, UK, 2002.

[13] Anonymous Traffic safety facts 2004: A compilation of motor vehicle crash data from the fatality analysis reporting system and the general estimates system. National Highway Traffic Safety Administration, National Center for Statistics and Analysis. U.S. Department of Transportation: Washington DC, USA. 2005.

[14] L. J. J. Kusters, "Increasing Rollover Safety of Commercial Vehicles by Application of Electronic Systems," *Smart Vehicles,* pp. 362-377, 1995.

[15] A. J. P. Miege and D. Cebon, "Active Roll Control of an Experimental Articulated Vehicle," *Journal of Automobile Engineering*, vol. 219, pp. 791-806, 2005.

[16] J. H. F. Woodrooffe, "Practical concepts in heavy truck rollover accident analysis," in Heavy Vehicles Rollovers Conference, Atlanta, USA, 1993.

[17] C. B. Winkler, R. D. Ervin and M. R. Hagan. *On-Board Estimation of Rollover Threshold of Tractor Semitrailers*. IAVSD, Pretoria, South Africa, 1999.

[18] E. C. von Glasner. Active safety of commercial vehicles. *JSAE Rev. 16(2),* pp. 211-211. 1995.

[19] L. Palkovics, A. Semsey and E. Gerum, "Roll-Over Prevention System for Commercial Vehicles – Additional Sensorless Function of the Electronic Brake System," *Vehicle System Dynamics,* vol. 32, pp. 285-297, 1999.

[20] P. S. Fancher, R. D. Ervin, C. B. Winkler and T. D. Gillespie. A factbook of the mechanical properties of the components for single-unit and articulated heavy trucks. technical report UMTRI-86-12. University of Michigan Transportation Research Institute. Ann Arbor, MI, USA. 1986.

[21] P. S. Fancher and A. Mathew, "A vehicle dynamics handbook for single-unit and articulated heavy trucks. technical report UMTRI-86-37," University of Michigan Transportation Research Institute, Ann Arbor, MI, USA, 1987.

[22] L. Segel. Course on the mechanics of heavy-duty trucks and truck combinations. Surfers Paradise, Old, Australia 1988. UMTRI

[23] F. Vlk. Lateral dynamics of commercial vehicle combinations. A literature survey. *Veh. Syst. Dyn. 11(305-324),* 1982.

[24] F. Vlk. Handling performance of truck-trailer vehicles: A state-of-the-art survey. *Int. J. Veh. Des. 6*pp. 323-361. 1985.

[25] A. Nalecz and J. Genin. Dynamic stability of heavy articulated vehicles. *Int. J. Veh. Des. 5*pp. 417-426. 1984.

[26] L. Segel and R. D. Ervin, "The influence of tire factors on the stability of trucks and truck-trailers," *Veh. Syst. Dyn.* vol. 10, pp. 39-59, 1981.

[27] J. R. Ellis. *Vehicle Handling Dynamics*. Wiley-Blackwell , 1994.

[28] C. B. Winkler. Simplified analysis of the steady-state turning of complex vehicles. *Veh. Syst. Dyn. 29(3),* pp. 141-180. 1998.

[29] H. B. Pacejka. Simplified analysis of steady-state turning behaviour of motor vehicles. part 1. handling diagrams of simple systems. *Veh. Syst. Dyn. 2(3),* pp. 161-172. 1973.

[30] H. B. Pacejka. Simplified analysis of steady-state turning behaviour of motor vehicles part 2: Stability of the steady-state turn. *Veh. Syst. Dyn. 2(4),* pp. 173-183. 1973.

[31] H. B. Pacejka. Simplified analysis of steady-state turning behaviour of motor vehicles part 3: More elaborate systems. *Veh. Syst. Dyn. 2(4),* pp. 185-204. 1973.

[32] T. D. Gillespie. *Fundamentals of Vehicle Dynamics*, SAE International, 1992.

[33] R. N. Kemp, B. P. Chinn and G. Brock, "Articulated vehicle roll stability: Method of assessment and effects of vehicle characteristics.technical report TRRL-788," Transport and Road Research Laboratory, UK, 1978.

[34] R. D. Ervin. *The Influence of Size and Weight Variables on the Roll Stability of Heavy Duty Trucks* 1983.

[35] P. W. Blow, J. H. Woodrooffe and P. F. Sweatman. Vehicle stability and control research for US comprehensive truck size and weight (TS&W) study. *SAE Transactions 107*pp. 617-623. 1998.

[36] D. Karnopp. Theoretical limitations in active vehicle suspensions. *Veh. Syst. Dyn. 15(1),* pp. 41-54. 1986.

[37] J. Hedrick and T. Butsuen. Invariant properties of automotive suspensions. *Proceedings of the Institution of Mechanical Engineers, Part D: Journal of Automobile Engineering 204(14),* pp. 21-27. 1990.

[38] M. C. Smith. Achievable dynamic response for automotive active suspensions. *Veh. Syst. Dyn. 24(1),* pp. 1-34. 1995.

[39] R. J. Dorling, "Integrated Control of Road Vehicle Dynamics," PhD thesis, University of Cambridge, UK, 1996.

[40] G. W. Walker. Constraints upon the achievable performance of vehicle suspension systems. PhD thesis, University of Cambridge, UK, 1997.

[41] M. C. Smith and G. W. Walker. Performance limitations and constraints for active and passive suspensions: A mechanical multi-port approach. *Veh. Syst. Dyn. 33(3),* pp. 137-168. 2000.

[42] R. Sharp and S. Hassan. Performance and design considerations for dissipative semi-active suspension systems for automobiles. *Proceedings of the Institution of Mechanical Engineers 201(24),* pp. 149-153. 1987.

[43] R. Sharp and S. Hassan. The relative performance capabilities of passive, active and semi-active car suspension systems. *Proceedings of the Institution of Mechanical Engineers 200(34),* pp. 219-228. 1986.

[44] R. Sharp and S. Hassan. On the performance capabilities of active automobile suspension systems of limited bandwidth. *Veh. Syst. Dyn. 16(4),* pp. 213-225. 1987.

[45] D. Karnopp. Are active suspensions really necessary? In *Proc. ASME Winter Annual Meeting, Dynamic Systems and Control Division*, pp. 1-9, 1978.

[46] B. K. Chance, "Continental Mark VII/Lincoln Continental Electronically Controlled Air-Suspension (EAS) System," SAE, 840342 (1984).

[47] M. Mizuguchi, T. Suda, S. Chikamori and K. Kobayashi, "Chassis electronic control systems for the Mitsubishi 1894 Galant," SAE, 881133 (1984).

[48] Y. Yokoya, K. Asami, T. Hamajima and N. Nakashima, "Toyota electronic modulated suspension (TEMS) system for the 1983 Soarer," SAE, 840341 (1984).

[49] B. Acker, W. Darenberg and H. Gall. Active suspension for passenger cars. *IAVSD 89*pp. 15-25. 1989.

[50] Y. Aoyam, K. Kawabata, S. Hasegawa, Y. Kobari, M. Sato and E. Tsuruta, Development of the fully active suspension by Nissan. SAE, 901747 (1990).

[51] P. G. Wright and D. A. Williams, "An application of the active suspension to high performance road vehicles," *Inst. Mech. Engrs., C239/84,* 1984.

[52] J. Dominy and D. Bulman. An active suspension for a formula one grand prix racing car. *Journal of Dynamic Systems, Measurement, and Control 107*pp. 73. 1985.

[53] E. C. Von Glasner, E. Göhring, R. Povel and P. Schützner. Analysis of intelligent suspension systems for commercial vehicles. *SAE Transactions 102*pp. 896-896. 1993.

[54] D. Furleigh, M. Vanderploeg and C. Oh, Multiple steered axles for reducing the rollover risks of heavy articulated trucks. SAE, 881866 (1988).

[55] C. Cheng. Enhancing safety of actively-steered articulated vehicles. PhD thesis, University of Cambridge, UK, 2009.

[56] C. R. Carlson and J. C. Gerdes. Optimal rollover prevention with steer by wire and differential braking. Presented at Proceedings of IMECE. 2003, .

[57] P. Frank, L. Palkovics and P. Gianone. Using wheel speed and wheel slip information for controlling vehicle chassis systems. Presented at Proc. 5th International Symposium on Advanced Vehicle Control. 2000, .

[58] A. Lewis and M. El-Gindy. Sliding mode control for rollover prevention of heavy vehicles based on lateral acceleration. *International Journal of Heavy Vehicle Systems 10(1),* pp. 9-34. 2003.

[59] P. Gáspár, I. Szaszi and J. Bokor. Two strategies for reducing the rollover risk of heavy vehicles. *Periodica Polytecnica Ser.Transp.Eng 33(1-2),* pp. 139-147. 2005.

[60] A. B. Dunwoody and S. Froese. Active roll control of a semi-trailer. *SAE Transactions 102*pp. 999-999. 1993.

[61] R. C. Lin, D. Cebon and D. J. Cole. An investigation of active roll control of heavy road vehicles. *Veh. Syst. Dyn. 23*pp. 308-321. 1994.

[62] R. C. Lin, D. Cebon and D. J. Cole. Active roll control of articulated vehicles. *Veh. Syst. Dyn. 26(1),* pp. 17-43. 1996.

[63] R. C. Lin, D. Cebon and D. J. Cole. Optimal roll control of a single-unit lorry. *Proceedings of the Institution of Mechanical Engineers, Part D: Journal of Automobile Engineering 210(14),* pp. 45-55. 1996.

[64] D. J. M. Sampson. Active roll control of articulated heavy vehicles. PhD thesis, University of Cambridge, UK, 2000.

[65] A. J. P. Miege, "Active Roll Control of an Experimental Articulated Vehicle," PhD thesis, University of Cambridge, UK, 2003.

[66] J. Aurell and S. Edlund. The influence of steered axles on the dynamic stability of heavy vehicles. *SAE Paper 8924981*989.

[67] A. Odhams, R. Roebuck, D. Cebon and C. B. Winkler. Dynamic safety of active trailer steering systems. *Proceedings of the Institution of Mechanical Engineers, Part K: Journal of Multi-Body Dynamics 222(4),* pp. 367. 2008.

[68] K. Rangavajhula and H. S. J. Tsao. Command steering of trailers and command-steering-based optimal control of an articulated system for tractor-track following. *Proc. Inst. Mech. Eng. Pt. D: J. Automobile Eng. 222(6),* pp. 935-954. 2008.

[69] K. Rangavajhula and H. S. J. Tsao. Active trailer steering control of an articulated system with a tractor and three full trailers for tractor-track following. *International Journal of Heavy Vehicle Systems 14(3),* pp. 271-293. 2007.

[70] M. M. Islam and Y. He. Stability optimization of articulated frame steer vehicles. 2nd CIRP Conference on Assembly Technologies and Systems. Toronto, Canada, 2008, .

[71] M. Islam and Y. He. Design synthesis of heavy articulated vehicles with rearward amplification control. Presented at Proceedings of the 22 Nd Canadian Congress of Applied Mechanics, Dalhousie University, Halifax, Canada. 2009, .

[72] Y. He, M. M. Islam and T. D. Webster. An integrated design method for articulated heavy vehicles with active trailer steering systems. *SAE International Journal of Passenger Cars-Mechanical Systems 3(1),* pp. 158. 2010.

[73] M. M. Islam, Y. He and T. D. Webster. Automated design synthesis of articulated heavy vehicles with active trailer steering systems. 2010, .

[74] W. Kortüm. Review of multibody computer codes for vehicle system dynamics. *Veh. Syst. Dyn. 22(S1),* pp. 3-31. 1993.

[75] M. W. Sayers, "Vehicle models for RTS applications," in 1998, pp. 541-546.

[76] M. W. Sayers. Symbolic computer methods to automatically formulate vehicle simulation codes. 1990.

[77] B. A. Suresh and B. J. Gilmore. Vehicle model complexity-how much is too much? *Quality and Design Issues in Automotive Simultaneous Engineering* 1994.

[78] M. W. Sayers and S. M. Riley. Modeling assumptions for realistic multibody simulations of the yaw and roll behavior of heavy trucks. *SAE Transactions 105*pp. 72-83. 1996.

[79] R. I. King and D. A. Crolla, "Flexible and efficient model development and analysis for road vehicle dynamics using a modular approach," in 1998, pp. 547-551.

[80] Anonymous *Merriam-Webster Dictionary* [http://www.merriam-webster.com/].

[81] E. G. Talbi. *Metaheuristics: From Design to Implementation*. Wiley, 2009.

[82] F. Glover. Future paths for integer programming and artificial intelligence. *Comput. Oper. Res. 13*pp. 533–549. 1986.

[83] M. Gen and R. Cheng. *Genetic Algorithms and Engineering Optimization*. Wiley, 2000.

[84] C. Mares and C. Surace. An application of genetic algorithms to identify damage in elastic structures. *J. Sound Vibrat. 195(2),* pp. 195-215. 1996.

[85] S. Forrest. Genetic algorithms: Principles of natural selection applied to computation. *Science 261(5123),* pp. 872. 1993.

[86] R. E. Kalman. Contributions to the theory of optimal control. *Bol.Soc.Mat.Mexicana 5(2),* pp. 102-119. 1960.

[87] R. E. Kalman. *When is a Linear Control System Optimal?* (1963). ASME transactions Series D (Journal of Basic Engineering), 51-60.

[88] F. Lin. *Robust Control Design: An Optimal Control Approach*, Wiley, 2007.

[89] S. H. Zak. *Systems and Control*, Oxford University Press, 2003.

[90] D. H. Wu and J. Hai. Analysis of dynamic lateral response for a multi-axle-steering tractor and trailer. *International Journal of Heavy Vehicle Systems 10(4),* pp. 281-294. 2003.

[91] Anonymous *Road Vehicles–Heavy Commercial Vehicle Combinations and Articulated Buses-Lateral Stability Test Methods.* Geneva, Switzerland: International Organization for Standardization, 12p. ISO 14790:2000(E).

[92] Anonymous A test for evaluating the rearward amplification of multi-articulated vehicles. Standard J2179, Society of Automotive Engineers, September 1993.

[93] M. M. Islam, "Design Synthesis of Articulated Heavy Vehicles with Active Trailer Steering Systems," MASc thesis, University of Ontario Institute of Technology, Ontario, Canada, 2010.

[94] B. Jujnovich and D. Cebon. Comparative performance of semi-trailer steering systems. Presented at Proceedings of the Seventh International Symposium on Heavy Vehicle Weights and Dimensions. 2002, .

[95] R. C. Lin, "An investigation of active roll control for heavy vehicle suspensions," PhD thesis, University of Cambridge, UK, 1994.

[96] T. D. Gillespie and C. MacAdam. Constant velocity Yaw/Roll program User's manual. University of Michigan Transportation Research Institute, Ann Arbor, USA, 1982.

[97] D. Oberoi, M. M. Islam and Y. He, "Design optimization of articulated heavy vehicles using genetic algorithms and multibody vehicle models," in *Proc. of 23rd Canadian Congress of Applied Mechanics*, 2011, .

[98] D. Oberoi and Y. He, "Simulation-based design synthesis of articulated heavy vehicles for improving maneuverability and stability," in *Proc. of 4th International Conference on Mechanical Engineering and Mechanics*, 2011, .

[99] Y. He, "Design of Rail Vehicles with Passive and Active Suspensions Using Multidisciplinary Optimization, Multibody Dynamics, and Genetic Algorithms," PhD thesis, University of Waterloo, Ontario, Canada, 2003.

[100] Anonymous "TruckSim User Manual Version 8," Mechanical Simulation, Ann Arbor, Michigan, USA, 2009.

APPENDIX A

A.1 LINEAR VEHICLE MODEL SYSTEM MATRICES

State-space matrices for 5-DOF linear vehicle model

$$\dot{x} = Ax + Bu + C\delta$$

where $x = [\Phi_1\ \dot{\Phi}_1\ \beta_1\ \dot{\Psi}_1\ \Phi_2\ \dot{\Phi}_2\ \beta_2\ \dot{\Psi}_2\ \Phi_{t1}\ \Phi_{t2}]^T$ and $u = [u_{c1}\ u_{c2}]^T$

$$M = \begin{bmatrix} 0 & m_{12} & m_{13} & m_{14} & 0 & 0 & 0 & 0 & 0 & 0 \\ 0 & m_{22} & m_{23} & m_{24} & 0 & 0 & 0 & 0 & m_{29} & 0 \\ 0 & m_{32} & m_{33} & 0 & 0 & m_{36} & m_{37} & 0 & 0 & 0 \\ 0 & 0 & 0 & 0 & 0 & m_{46} & m_{47} & m_{48} & 0 & 0 \\ 0 & 0 & 0 & 0 & 0 & m_{56} & m_{57} & m_{58} & 0 & m_{510} \\ 0 & m_{62} & m_{63} & m_{64} & 0 & m_{66} & m_{67} & m_{68} & 0 & 0 \\ 0 & 0 & 0 & 0 & 0 & 0 & 0 & 0 & m_{79} & 0 \\ 0 & 0 & 0 & 0 & 0 & 0 & 0 & 0 & 0 & m_{810} \\ m_{91} & 0 & 0 & 0 & 0 & 0 & 0 & 0 & 0 & 0 \\ 0 & 0 & 0 & 0 & m_{105} & 0 & 0 & 0 & 0 & 0 \end{bmatrix}$$

$$N = \begin{bmatrix} 0 & 0 & n_{13} & n_{14} & 0 & 0 & 0 & 0 & 0 & 0 \\ n_{21} & n_{22} & n_{23} & n_{24} & n_{25} & 0 & 0 & 0 & n_{29} & 0 \\ 0 & 0 & n_{33} & n_{34} & 0 & 0 & n_{37} & n_{38} & 0 & 0 \\ 0 & 0 & 0 & 0 & 0 & 0 & n_{47} & n_{48} & 0 & 0 \\ n_{51} & 0 & 0 & 0 & n_{55} & n_{56} & n_{57} & n_{58} & 0 & n_{510} \\ 0 & 0 & 0 & n_{64} & 0 & 0 & 0 & n_{68} & 0 & 0 \\ n_{71} & n_{72} & 0 & 0 & 0 & 0 & 0 & 0 & n_{79} & 0 \\ 0 & 0 & 0 & 0 & n_{85} & n_{86} & 0 & 0 & 0 & n_{810} \\ 0 & n_{92} & 0 & 0 & 0 & 0 & 0 & 0 & 0 & 0 \\ 0 & 0 & 0 & 0 & 0 & n_{106} & 0 & 0 & 0 & 0 \end{bmatrix}$$

$$G = \begin{bmatrix} 0 & -1 & 0 & 0 & 0 & 0 & -1 & 0 & 0 & 0 \\ 0 & 0 & 0 & 0 & -1 & 0 & 0 & -1 & 0 & 0 \end{bmatrix}^T$$

$$D = [d_{11} \quad d_{12} \quad d_{13} \quad 0 \quad 0 \quad 0 \quad 0 \quad 0 \quad 0 \quad 0]^T$$

$$A = M^{-1}N$$

$$B = M^{-1}G$$

$$C = M^{-1}D$$

In matrices *M*, *N* and *D*, the relevant elements are given as:

$$m_{12} = -m_{s1}h_{s1}l_{c1} + m_{s1}h_{r1}l_{c1} - I_{xz1}$$

$$m_{13} = m_1u_1l_{c1}$$

$$m_{14} = I_{zz1}$$

$$m_{22} = I_{xx1} - 4m_{s1}h_{s1}h_{r1} - m_{s1}h_{s1}h_{cr1} + m_{s1}h_{r1}h_{cr1} + 2m_{s1}{h_{r1}}^2 + 2m_{s1}{h_{s1}}^2$$

$$m_{23} = m_{s1}u_1h_{r1} - m_{s1}u_1h_{s1} + m_1u_1h_{cr1}$$

$$m_{24} = -I_{xz1}$$

$$m_{29} = -L_{r1} - L_{f1}$$

$$m_{32} = -m_{s1}h_{s1} + m_{s1}h_{r1}$$

$$m_{33} = m_1u_1$$

$$m_{36} = -m_{s2}h_{s2} + m_{s2}h_{r2}$$

$$m_{37} = m_2u_2$$

$$m_{46} = l_{c2}m_{s2}h_{s2} - l_{c2}m_{s2}h_{r2} - I_{xz2}$$

$$m_{47} = -l_{c2}m_2u_2$$

$$m_{48} = I_{zz2}$$

$$m_{56} = 2m_{s2}{h_{r2}}^2 - 4m_{s2}h_{s2}h_{r2} + I_{xx2} + 2m_{s2}{h_{s2}}^2 - h_{cr2}m_{s2}h_{s2} + h_{cr2}m_{s2}h_{r2}$$

$$m_{57} = h_{cr2}m_2u_2 - m_{s2}u_2h_{s2} + m_{s2}u_2h_{r2}$$

$$m_{58} = -I_{xz2}$$

$$m_{510} = -L_{r2}$$

$$m_{62} = -\frac{h_{c1}}{u_1} + \frac{h_{r1}}{u_1}$$

$$m_{63} = 1$$

$$m_{64} = -\frac{l_{c1}}{u_1}$$

$$m_{66} = \frac{h_{c2}}{u_2} - \frac{h_{r2}}{u_2}$$

$$m_{67} = -1$$

$$m_{68} = -\frac{l_{c2}}{u_2}$$

$$m_{79} = -L_{f1} - L_{r1}$$

$$m_{810} = -L_{r2}$$

$$m_{91} = 1$$

$$m_{105} = 1$$

$$n_{13} = -N_{\beta 1} - Y_{\beta 1} l_{c1}$$

$$n_{14} = m_1 u_1 l_{c1} - Y_{r1} l_{c1} - N_{r1}$$

$$n_{21} = K_{12} + K_{f1} + K_{r1} - m_{s1} g h_{s1} + m_{s1} g h_{r1}$$

$$n_{22} = L_{f1} + L_{r1}$$

$$n_{23} = -Y_{\beta 1} h_{cr1}$$

$$n_{24} = m_{s1} u_1 h_{r1} - Y_{r1} h_{cr1} + m_1 u_1 h_{cr1} - m_{s1} u_1 h_{s1}$$

$$n_{25} = -K_{12}$$

$$n_{29} = -K_{f1} - K_{r1}$$

$$n_{33} = -Y_{\beta 1}$$

$$n_{34} = m_1 u_1 - Y_{r1}$$

$$n_{37} = -Y_{\beta 2}$$

$$n_{38} = -Y_{r2} + m_2 u_2$$

$$n_{47} = -N_{\beta 2} + l_{c2} Y_{\beta 2}$$

$$n_{48} = -l_{c2} m_2 u_2 - N_{r2} + l_{c2} Y_{r2}$$

$$n_{51} = -K_{12}$$

$$n_{55} = K_{r1} - m_{s2} g h_{s2} + m_{s2} g h_{r2} + K_{12}$$

$$n_{56} = L_{r2}$$

$$n_{57} = -h_{cr2}Y_{\beta 2}$$

$$n_{58} = m_{s2}u_2h_{r2} - h_{cr2}Y_{r2} + h_{cr2}m_2u_2 - m_{s2}u_2h_{s2}$$

$$n_{510} = -K_{r2}$$

$$n_{64} = 1$$

$$n_{68} = -1$$

$$n_{71} = K_{f1} + K_{r1}$$

$$n_{72} = L_{f1} + L_{r1}$$

$$n_{79} = -K_{f1} - K_{tr1} - K_{r1} - K_{tf1}$$

$$n_{85} = K_{r2}$$

$$n_{86} = L_{r2}$$

$$n_{810} = -K_{r2} - K_{tr2}$$

$$n_{92} = -1$$

$$n_{106} = -1$$

$$d_{11} = -Y_{\delta 1f}l_{c1} - N_{\delta 1f}$$

$$d_{12} = -Y_{\delta 1f}h_{cr2}$$

$$d_{13} = -Y_{\delta 1f}$$

where,

$$Y_{\beta 1} = c_{f1} + c_{r1}$$

$$Y_{r1} = \frac{c_{f1}a_1 - c_{r1}b_1}{u_1}$$

$$Y_{\delta 1f} = -c_{f1}$$

$$N_{\beta 1} = c_{f1}a_1 - c_{r1}b_1$$

$$N_{r1} = \frac{c_{f1}{a_1}^2 + c_{r1}{b_1}^2}{u_1}$$

$$N_{\delta 1f} = -c_{f1}a_1$$

$$Y_{\beta 2} = c_{r2}$$

$$Y_{r2} = \frac{-c_{r2}b_2}{u_2}$$

$$N_{\beta 2} = -c_{r2}b_2$$

$$N_{r2} = \frac{c_{r2}{b_2}^2}{u_2}$$

A.2 LQR WEIGHT MATRICES

$$Q = \begin{bmatrix} 10^{11} & 0 & 0 & 0 & 0 & 0 & 0 & 0 & 0 & 0 \\ 0 & 1 & 0 & 0 & 0 & 0 & 0 & 0 & 0 & 0 \\ 0 & 0 & 1 & 0 & 0 & 0 & 0 & 0 & 0 & 0 \\ 0 & 0 & 0 & 1 & 0 & 0 & 0 & 0 & 0 & 0 \\ 0 & 0 & 0 & 0 & 10^{14} & 0 & 0 & 0 & 0 & 0 \\ 0 & 0 & 0 & 0 & 0 & 1 & 0 & 0 & 0 & 0 \\ 0 & 0 & 0 & 0 & 0 & 0 & 1 & 0 & 0 & 0 \\ 0 & 0 & 0 & 0 & 0 & 0 & 0 & 1 & 0 & 0 \\ 0 & 0 & 0 & 0 & 0 & 0 & 0 & 0 & 1 & 0 \\ 0 & 0 & 0 & 0 & 0 & 0 & 0 & 0 & 0 & 1 \end{bmatrix}$$

$$R = \begin{bmatrix} 200 & 0 \\ 0 & 100 \end{bmatrix}$$

APPENDIX B

B.1 PARAMETERS USED IN CHAPTER 4

B.1.1 TRACTOR UNIT [55, 62, 100]

B.1.1.1 SPRUNG MASS AND OVERALL DIMENSIONS

Parameter	Value
Sprung Mass (m_{s1})	6179 kg
Roll Inertia (I_{xx1})	2411 kgm^2
Pitch Inertia (I_{yy1})	35408 kgm^2
Yaw Inertia (I_{zz1})	34823 kgm^2
Product (I_{xy1})	0 kgm^2
Product (I_{yz1})	0 kgm^2
Product (I_{xz1})	1626 kgm^2
Distance Front Wheel Centre–Sprung Mass CG (a_1)	710.2 mm
Distance Rear Wheel Centre–Sprung Mass CG (b_1)	2989.8 mm
Wheel Base (l_1)	3700 mm
Whole Mass CG Height (above ground) (h_{s1})	1173 mm

B.1.1.2 FRONT AXLE

Parameter	Value
Unsprung Mass (m_{u1})	527 kg
Roll & Yaw Inertia	612 kgm^2
CG Height (above ground)	500 mm
Roll Centre Height (above ground) (h_{r1})	695 mm
Track (t_1)	2022 mm
Steering Ratio	1:1
King-Pin Lateral Inclination	7.2^0
Castor Angle	5.2^0
Spring Rate	190 kN/m
Spring Centres	828 mm
Ratio Spring–Axle Compression	1:1
Damping Rate	30 kNs/m
Damper Centres	828 mm
Ratio Damper–Axle Compression	1:1
Auxiliary Roll Stiffness (K_{f1})	1100 Nm/deg
Auxiliary Roll Damping (L_{f1})	3500 Nms/deg
Combined Roll Stiffness (K_{tf1})	2.05 MNm/deg
Combined Cornering Stiffness (c_{f1})	-8.21633 kN/deg

B.1.1.3 REAR AXLE

Parameter	Value
Unsprung Mass (m_{u2})	1004 kg
Roll & Yaw Inertia	579 kgm^2
CG Height (above ground)	500 mm
Roll Centre Height (above ground) (h_{r1})	695 mm
Track (t_2)	1829 mm
Dual Tire Spacing	337 mm
Spring Rate	179 kN/m
Spring Centres	750 mm
Ratio Spring–Axle Compression	1.75:1
Damping Rate	40 kNs/m
Damper Centres	900 mm
Ratio Damper–Axle Compression	0.5:1
Auxiliary Roll Stiffness (K_{r1})	7850 Nm/deg
Auxiliary Roll Damping (L_{r1})	3500 Nms/deg
Combined Roll Stiffness (K_{tr1})	2.05 MNm/deg
Combined Cornering Stiffness (c_{r1})	-19.53777 kN/deg

B.1.1.4 TRACTOR TIRES

Parameter	Value
No. of Tires on Steer Axle	2
No. of Tires on Drive Axle	4
Rolling Radius	510 mm
Spring Rate	1500 kN/m
Coefficient of Friction	0.85

B.1.1.5 HITCH POINT

Parameter	Value
Distance Hitch Centre-Tractor Rear Wheel Centre	500 mm
Hitch Height (above ground)	1170 mm
Roll Stiffness (K_{12})	10 kNm/deg

B.1.2 SEMI-TRAILER UNIT [55, 62, 100]

B.1.2.1 SPRUNG MASS AND OVERALL DIMENSIONS

Parameter	Value
Sprung Mass (m_{s2})	29090 kg
Roll Inertia (I_{xx2})	20930 kgm^2
Pitch Inertia (I_{yy2})	390000 kgm^2
Yaw Inertia (I_{zz2})	413707 kgm^2
Product (I_{xy2})	0 kgm^2
Product (I_{yz2})	0 kgm^2
Product (I_{xz2})	0 kgm^2
Distance Hitch Centre–Sprung Mass CG (a_2)	5118.1 mm
Distance Rear Middle Wheel Centre–Sprung Mass CG (b_2)	2581.9 mm
Whole Mass CG Height (above ground) (h_{s2})	1600 mm
Wheel Base (l_2)	7700 mm
Axle Spacing	1430 mm

B.1.2.2 SEMI-TRAILER AXLES

Parameter	Value
Unsprung Mass (m_{u3})	735 kg
Roll & Yaw Inertia	593 kgm^2
CG Height (above ground)	520 mm
Roll Centre Height (above ground) (h_{r2})	715 mm
Track (t_3)	2140 mm
Spring Rate	179 kN/m
Spring Centres	750 mm
Ratio Spring–Axle Compression	1.75:1
Damping Rate	40 kNs/m
Damper Centres	900 mm
Ratio Damper–Axle Compression	0.5:1
Auxiliary Roll Stiffness (K_{r2})	15000 Nm/deg
Auxiliary Roll Damping (L_{r2})	8000 Nms/deg
Combined Roll Stiffness (K_{tr2})	6.1 MNm/deg
Combined Cornering Stiffness (c_{r2})	-28.95777 kN/deg

B.1.2.3 SEMI-TRAILER TIRES

Parameter	Value
No. of Tires per Trailer Axle	2
Rolling Radius	510 mm
Spring Rate	1500 kN/m
Coefficient of Friction	0.85

B.1.3 MISCELLANEOUS

Parameter	Value
Longitudinal Velocity ($u_1 = u_2$)	24.44 m/s
Acceleration due to Gravity (g)	9.81 m/s^2

B.2 PARAMETERS USED IN CHAPTER 5

B.2.1 TRACTOR UNIT [55, 62, 100]

B.2.1.1 SPRUNG MASS AND OVERALL DIMENSIONS

Parameter	Value
Sprung Mass (m_{s1})	6179 kg
Roll Inertia (I_{xx1})	2411 kgm^2
Pitch Inertia (I_{yy1})	35408 kgm^2
Yaw Inertia (I_{zz1})	34823 kgm^2
Product (I_{xy1})	0 kgm^2
Product (I_{yz1})	0 kgm^2
Product (I_{xz1})	1626 kgm^2
Distance Front Wheel Centre–Sprung Mass CG (a_1)	710.2 mm
Distance Rear Wheel Centre–Sprung Mass CG (b_1)	2989.8 mm
Whole Mass CG Height (above ground) (h_{s1})	1173 mm
Wheel Base (l_1)	3700 mm

B.2.1.2 FRONT AXLE

Parameter	Value
Unsprung Mass (m_{u1})	527 kg
Roll & Yaw Inertia	612 kgm^2
CG Height (above ground)	500 mm
Roll Centre Height (above ground)	447 mm
Track (t_1)	2022 mm
Steering Ratio	25:1
King-Pin Lateral Inclination	7.2^0
Castor Angle	5.2^0
Spring Rate	190 kN/m
Spring Centres	828 mm
Ratio Spring–Axle Compression	1:1
Damping Rate	30 kNs/m
Damper Centres	828 mm
Ratio Damper–Axle Compression	1:1
Auxiliary Roll Stiffness (K_{f1})	1100 Nm/deg

B.2.1.3 REAR AXLE

Parameter	Value
Unsprung Mass (m_{u2})	1004 kg
Roll & Yaw Inertia	579 kgm^2
CG Height (above ground)	500 mm
Roll Centre Height (above ground)	695 mm
Track (t_2)	1829 mm
Dual Tire Spacing	337 mm
Spring Rate	246 kN/m
Spring Centres	760 mm
Ratio Spring–Axle Compression	1:1
Damping Rate	30 kNs/m
Damper Centres	800 mm
Ratio Damper–Axle Compression	0.5:1
Auxiliary Roll Stiffness (K_{r1})	7850 Nm/deg

B.2.1.4 TRACTOR TIRES

Parameter	Value
No. of Tires on Steer Axle	2
No. of Tires on Drive Axle	4
Rolling Radius	510 mm
Spring Rate	1500 kN/m
Coefficient of Friction	0.85

B.2.1.5 HITCH POINT

Parameter	Value
Distance Hitch Centre-Tractor Rear Wheel Centre	500 mm
Hitch Height (above ground)	1170 mm
Roll Stiffness (K_{12})	10 kNm/deg (Roll < 1 deg) 650 kNm/deg (Roll > 1 deg)

B.2.2 SEMI-TRAILER UNIT [55, 62, 100]

B.2.2.1 SPRUNG MASS AND OVERALL DIMENSIONS

Parameter	Value
Sprung Mass (m_{s2})	29090 kg
Roll Inertia (I_{xx2})	20930 kgm^2
Pitch Inertia (I_{yy2})	390000 kgm^2
Yaw Inertia (I_{zz2})	413707 kgm^2
Product (I_{xy2})	0 kgm^2
Product (I_{yz2})	0 kgm^2
Product (I_{xz2})	0 kgm^2
Distance Hitch Centre–Sprung Mass CG (a_2)	5118.1 mm
Distance Rear Middle Wheel Centre–Sprung Mass CG (b_2)	2581.9 mm
Whole Mass CG Height (above ground) (h_{s2})	1600 mm
Wheel Base (l_2)	7700 mm
Axle Spacing	1430 mm

B.2.2.2 SEMI-TRAILER AXLES

Parameter	Value
Unsprung Mass (m_{u3})	735 kg
Roll & Yaw Inertia	593 kgm^2
CG Height (above ground)	520 mm
Roll Centre Height (above ground)	715 mm
Track (t_3)	2140 mm
Spring Rate	179 kN/m
Spring Centres	750 mm
Ratio Spring–Axle Compression	1.75:1
Damping Rate	40 kNs/m
Damper Centres	900 mm
Ratio Damper–Axle Compression	0.5:1
Auxiliary Roll Stiffness (K_{r2})	15000 Nm/deg

B.2.2.3 SEMI-TRAILER TIRES

Parameter	Value
No. of Tires per Trailer Axle	2
Rolling Radius	510 mm
Spring Rate	1500 kN/m
Coefficient of Friction	0.85

B.2.3 DRIVER MODEL

Parameter	Value
Driver Preview Time	1.0 s
Driver Time Lag	0 s
Maximum Steering Wheel Angle	720 deg
Maximum Steering Wheel Angle Rate	1200 deg/s
Nominal Steering Gear Ratio	25:1

B.2.4 MISCELLANEOUS

Parameter	Value
Longitudinal Velocity (High Speed Single Lane Change)	24.44 m/s
Longitudinal Velocity (Swept Path Width 90^0 Turn)	1.38 m/s
Acceleration due to Gravity (g)	9.81 m/s^2